J Physiol 603.22 (2025) pp 7049–7070

The Journal of Physiology

High-frequency electrical tuning and linear filter properties of Knollenorgan electroreceptors of mormyrid electric fish

Indira M. Raman[1,2] and Carl D. Hopkins[1]

[1]*Department of Neurobiology and Behavior, Cornell University, Ithaca, New York, USA*
[2]*Department of Neurobiology, Northwestern University, Evanston, Illinois, USA*

Handling Editors: Katalin Toth & Samuel Young

The peer review history is available in the Supporting Information section of this article (https://doi.org/10.1113/JP288299#support-information-section).

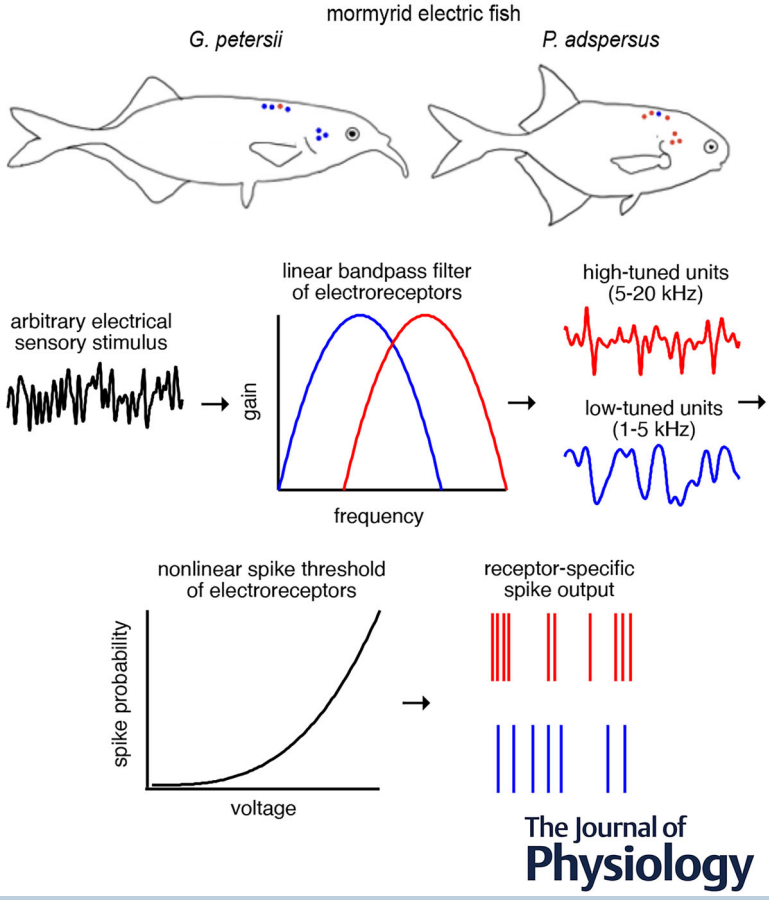

Abstract figure legend Knollenorgans of mormyrid fish transmit high-frequency electrical signals. Mormyrid electric fish (*top*) have Knollenorgans (electroreceptors) on their bodies (*red* and *blue dots*) that detect electrical stimuli (*middle, left*) through an electrical tuning mechanism. The receptors act as linear bandpass filters (*middle, centre*) that transduce different ranges of frequencies from about 1–20 kHz (*middle, right*). Rectification and non-linear thresholding (*bottom, left*) convert the responses to well-timed spikes (*bottom, right*), which vary across receptors but faithfully transmit signals well above 10 kHz.

DOI: 10.1113/JP288299

Abstract Electrical tuning allows auditory, vestibular, and electrosensory receptor cells to filter sensory signals and selectively transmit specific stimulus frequencies. In auditory hair cells, electrical tuning results from membrane potential resonance produced by voltage-gated Ca and K(Ca) channels, with variable kinetics that generate different tuning properties. Such resonance has been observed only up to ∼1 kHz, however. Additionally, in most species that employ electrical tuning, hearing is constrained to this relatively low-frequency range, raising the question of whether electrical tuning can extend to higher frequencies. Here we investigated this possibility by studying tuning and transduction properties of Knollenorgans, a class of tuberous electroreceptors of mormyrid electric fish. These organs, which generate spike-like receptor potentials, detect species-specific electric organ discharges (EODs). To test whether fish with brief EODs had correspondingly high-frequency electrical tuning, we recorded tuning curves from Knollenorgans of three species, *Brevimyrus niger, Gnathonemus petersii*, and *Pollimyrus adspersus*, which have EODs with spectral components exceeding 5 kHz. All species had receptors tuned to a range of frequencies tiling the species-specific EOD spectrum, with best frequencies extending beyond 10 kHz in *P. adspersus*. We also computed the impulse response of each Knollenorgan by reverse-correlating spikes elicited by white noise stimuli. After incorporation of a spike threshold non-linearity, convolving the impulse response with arbitrary stimulus waveforms successfully predicted spike patterns experimentally evoked by these inputs. These analyses demonstrate that differential electrical tuning properties of Knollenorgans produce distinct, well-timed spike responses that reliably encode time-varying electrical signals at frequencies up to 20 kHz.

(Received 3 December 2024; accepted after revision 21 May 2025; first published online 15 June 2025)
Corresponding author I. M. Raman: Department of Neurobiology, Northwestern University, 2205 Tech Drive, Evanston, IL 60208, USA. Email: i-raman@northwestern.edu

Key points

- Knollenorgans, among the tuberous electroreceptors of mormyrid electric fish, are modified hair cells that transduce electrical signals into spike-like receptor potentials.
- Knollenorgans in three species of mormyrids are tuned to frequencies matched to the frequencies present in the species-typical electric organ discharges, suiting them for electric communication.
- The frequency of highest sensitivity of Knollenorgans can extend well beyond 10 kHz, far exceeding the limit for electrical tuning mechanisms estimated from mechanosensitive hair cells.
- The timing and probability of spiking by Knollenorgans are accurately predicted by a model composed of linear filtering followed by non-linear rectification and spike thresholding.
- Differential filtering by different Knollenorgans produces distinct outputs to the same input, with high-tuned receptors effectively transmitting well-timed spikes, on a microsecond time scale, in response to electrical stimuli up to 20 kHz.

At the time of experimentation for this project, **Indira M. Raman** was an undergraduate in the laboratory of Professor Carl D. Hopkins at Cornell University. She is currently the Bill and Gayle Cook Professor of Biological Sciences and Chair of the Department of Neurobiology at Northwestern University. She has conducted research on electrophysiological and synaptic specializations that contribute to well-timed neural signalling in the cerebellum, auditory system, and electrosensory system.

Introduction

Sensory receptors of many sensory modalities act as filters, transducing and transmitting only a subset of attributes of any incoming sensory signal. Auditory and vestibular hair cells, for example, are particularly well known for their sharp tuning properties (Crawford & Fettiplace, 1980; Fettiplace, 2020; Hudspeth & Lewis, 1988a, 1988b). In these sensory cells, the ability to transmit a narrow band of frequencies stems both from mechanical tuning, initiated for auditory hair cells by the basilar membrane and amplified in mammals and birds by piezoelectric effects in outer/short hair cells (Békésy, 1960; Beurg et al., 2013; Dallos & Evans, 1995; Zheng et al., 2000), and from electrical tuning, resulting from properties of ion channels expressed in hair cell bodies (Art et al., 1986; Crawford & Fettiplace, 1980, 1981; Fettiplace, 2020; Fettiplace & Crawford, 1980; Hudspeth & Lewis, 1988a, 1988b; Ramanathan et al., 1999). Unlike mechanical tuning, which is present across vertebrates, electrical tuning has been described primarily in non-mammalian species, including turtle, frog, alligator, chick and gecko (Crawford & Fettiplace, 1981; Fuchs & Evans, 1988; Fuchs et al., 1988; Pitchford & Ashmore, 1987; Smotherman & Narins, 1999; Tan et al., 2013), in which hearing is largely restricted to frequencies below a few kilohertz. Moreover, direct recordings from hair cells suggest an upper limit for ion-channel-mediated electrical resonance of ∼2 kHz (Fettiplace, 2020; Tan et al., 2013). These data raise the question of whether this limited range reflects biophysical constraints on the ability of electrical tuning to encode higher frequencies effectively.

Testing the dynamic range of electrical tuning with auditory or vestibular hair cells, however, is complicated by the nature of the stimulus, which necessarily introduces a mechanical component into the transduction process. Electrosensory receptors of mormyrid electric fish, by contrast, provide a viable alternative, as the natural stimulus that they detect is electrical. These fish generate pulse-like electric organ discharges (EODs) that communicate species, sex, territoriality, courtship and possibly individual identity (Bass & Hopkins, 1984; Hopkins & Bass, 1981). EODs are brief mono-, bi- or triphasic signals composed of frequencies in the kilohertz range, i.e. 2–4 orders of magnitude higher than the 1–10 Hz signals detected during passive electrolocation (Hopkins, 1988), suggesting that any EOD-sensitive electroreceptors must be able to detect such high frequencies. Among the multiple classes of electroreceptor distributed over the bodies of mormyrid fish (Harder, 1968; Quinet, 1971), ampullary receptors and tuberous mormyromasts detect the low frequencies associated with passive and active electrolocation, respectively (Bell, 1989; Bennett, 1965; Hopkins, 1981). By contrast Knollenorgans, another class of tuberous electroreceptors, detect and encode the EODs of conspecifics (Bass & Hopkins, 1984; Friedman & Hopkins, 1998; Hopkins & Bass, 1981; Zipser & Bennett, 1976). Each Knollenorgan is composed of one to five modified hair cells encased by a fibrous wall, insulated by desmosomes and covered by loosely packed epithelial cells (Derbin & Szabo, 1968). Because they transduce electrical sensory signals from the external world into electrical neuronal signals of the nervous system, no mechanical steps are required, and any filtering that occurs is highly likely to result from electrical processes. Knollenorgans thus emerge as an ideal point of entry for studying the properties and capacity of high-frequency electrical tuning in sensory transduction.

Here we investigated the electrical tuning properties of Knollenorgans by making non-invasive extracellular recordings from three species of mormyrid fish: *Brevimyrus niger* (Günther, 1866), *Gnathonemus petersii* (Günther, 1862) and *Pollimyrus adspersus* (Günther, 1866). By recording spike-like receptor potential responses to sinusoidal electrical stimuli over a range of frequencies, we measured tuning curves for individual Knollenorgans. We also assessed the linear and non-linear components of the transduction process by applying Gaussian noise stimuli to estimate the impulse response of each Knollenorgan and then quantifying the extent to which the impulse response could predict the tuning curve and the response to arbitrary electrical stimuli. The data reveal tuning curves with best frequencies well above 5 kHz in Knollenorgans of all species, extending as high as 15 kHz in *P. adspersus*. Consistent with encoding communication signals, the range of tuning curves in each species overlaps with the frequencies present in the species-specific EOD. Finally the spiking patterns of individual Knollenorgans are predictable from the impulse response, with high-tuned receptors effectively transmitting electrical signals up to 20 kHz.

Methods

Ethical approval

All experiments were conducted at Cornell University in 1987–1988 as an undergraduate research project. The data were analysed but unpublished, except three tuning curves later reproduced in a review article (Wu et al., 1995). The raw data were fully preserved. Recent interest in electrical tuning (Bellono et al., 2017, 2018; Beurg et al., 2022; Fettiplace, 2020) led us to re-analyse the original dataset, informed by current research questions.

At the time that experiments were conducted institutional ethical approval for experiments on fish was not required. The experiments fully complied with the regulatory requirements of the period. Procedures were reviewed and approved by the NIH (MH37972,

to C.D.H.), and experiments were performed with attention to the well-being and viability of the fish. The consideration of this work has been approved by the Editor-in-Chief and the Ethics Editor of the *Journal of Physiology*. The investigators understand the ethical principles under which the journal operates.

Animals

Experiments were performed on three species of mormyrid electric fish that inhabit the Niger River basin: *B. niger*, *G. petersii*, and *P. adspersus*. Fish were imported from West Africa by commercial dealers and socially housed in 400-l tanks, with water conductivity maintained just below 200 μS/cm. Fish were fed live blackworms and were kept on a 12-h light /dark cycle.

The species were identified based on published descriptions of *B. niger* (Daget, 1954), *G. petersii* (Boulenger, 1909) or *P. adspersus* (Bigorne, 1990, 2003; Blache, 1964; Boulenger, 1909). Because EODs are the same for both sexes in the immature specimens of *B. niger* and *G. petersii* used here, no attempt was made to identify sex in these species. For *P. adspersus* sex was identified by the notch in the base of the anal fin present in males (Nawar, 1959; see also Pezzanite & Moller, 1998; Saunders & Gallant, 2024), as well as by the sexually dimorphic EOD waveform. Experiments were performed on eight specimens of *B. niger*, three *G. petersii* and seven *P. adspersus*. All *P. adspersus* specimens available for experimentation turned out to be male.

Each fish was immobilized for the duration of the experiment with flaxedil (20 μl at 0.25 mg/ml) s.c.), which also silenced the fish's own EOD. The fish was placed in a small tank filled with aquarium water (maintained at 25°C–27°C) where it rested on a Plexiglas block and was held in place by adjustable Plexiglas rods. The fish was respired through the mouth with aerated water. Throughout the experiment it was repeatedly checked to ensure that the water continued to flow through its gills. After the experiment the fish recovered from the flaxedil over a period of a few hours and then was returned to its home aquarium. No fish was used for multiple experiments.

Electrophysiological recordings

Knollenorgans in immobilized fish were identified visually under a dissecting microscope as reddish spots measuring 150–300 μm in diameter (Bennett, 1965). A 0.7 mm diameter glass capillary containing an Ag/AgCl electrode and aquarium water was positioned perpendicularly over the Knollenorgan pore, and a bridge amplifier (WPI M-707) was used for extracellular stimulation and recording through the same electrode. A 2 × 1 cm Ag/AgCl ground electrode was placed in the tank about 10 cm from the fish. Each Knollenorgan was electrically stimulated with noise or a 1 kHz test tone, and only those units that responded with spikes with a high signal-to-noise ratio on the oscilloscope trace were studied further. Stimulus artefact generated in the stimulating-recording probe was balanced within the amplifier by subtraction of an attenuated and phase-shifted stimulus copy from the response.

After recording, the position of each Knollenorgan was mapped onto a large portrait of a specimen of the species. All recordings were made from receptors above the mid-line on the right side of the fish.

Tuning curves. Frequency tuning curves were generated with a waveform generator (Wavetek 175) controlled by a PDP 11/34 computer. The stimulus waveform was transmitted to the electrode through an attenuator (Hewlett-Packard 350-D), a summing amplifier (Tektronix) and the bridge amplifier. Both the stimulus waveform and the spike-like receptor potential responses were monitored on a dual-trace oscilloscope.

To generate the frequency tuning curve, the Knollenorgan was stimulated at each frequency with three 100 ms sine wave bursts shaped by a trapezoidal ramp function with 5 ms rise and fall time. The stimulus strength could range from peak-to-peak sine wave of 5 μA (0 dB attenuation) to 0.5 nA (80 dB attenuation). The initial stimulus strength was 5 nA (40 dB attenuation). The intensity of the stimulus was automatically varied to find the threshold stimulus, defined as the lowest intensity necessary to elicit a predetermined criterion number of spikes above than the spontaneous rate measured in the absence of stimulation. For Knollenorgans with spontaneous rates <90 spikes/s, threshold was set at 1 spike/100 ms (an increase of 10 spikes/s); for three units with spontaneous rates >100 spikes/s, threshold was set at 2 spikes/100 ms (20 spikes/s). If the spike rate exceeded the criterion, the stimulus strength was decreased by 0.5 dB until the response fell below criterion, at which point the previous stimulus amplitude, measured in dB attenuation, was accepted as threshold. Each Knollenorgan was stimulated at 100 or more frequencies covering about 2.5 log units between 0.1 and 25.0 kHz at equal intervals on a log scale, starting with the lowest and increasing to the highest frequency.

Stimulation with white noise and reverse correlation. To determine the spike triggered reverse average as an estimate of the impulse response each Knollenorgan was stimulated with 30 s of pseudo-random Gaussian white noise, prepared by producing an 8000 word sequence of random numbers with a Gaussian distribution down-loaded into the arbitrary waveform generator (Wavetek),

sampled at 10 μs/point. The noise was low-pass filtered (24 dB/octave, Krohn-Hite 3202) at 10 kHz for *B. niger* and *G. petersii* and 20 kHz for *P. adspersus*.

The noise was attenuated enough to decrease the stimulus artefact that could not be balanced, while still producing a response of spikes above the spontaneous rate. Spikes were converted to square wave trigger pulses by a Schmitt trigger. The noise and the trigger pulses were recorded on separate channels of a tape recorder (Lockheed Store 4, FM mode), with a tape speed of 60 inches/s.

Noise-evoked PSTHs. Peristimulus time histograms (PSTHs) of spikes were generated by stimulating Knollenorgans with 10.24 ms segments of noise filtered at 10, 5, or 2.5 kHz for *B. niger* and *G. petersii* or 20 kHz for *P. adspersus*. Each noise stimulus was preceded by a calibration step. Stimuli were applied 2000 times, and the Schmitt trigger square wave responses were recorded. The stimulus was then inverted and applied 2000 more times. PSTHs to 'upright' and 'inverted' noise stimuli were made with 20 μs bins and summed to obtain the compound PSTH. In a subset of Knollenorgans from *P. adspersus* (KO73, KO74, KO77, see *Results*), the 20 kHz noise segment was 2.048 ms long, applied 4000 times with each polarity, and PSTHs were constructed with 4 μs bins.

EODs. EODs used for comparisons were previously recorded in the laboratory and kindly provided by G. Harned (*B. niger, G. petersii*) and J.D. Crawford (*P. adspersus*). Spontaneously generated EODs were recorded with Ag-AgCl electrodes from individual fish freely swimming in aquarium water in a small holding tank. EODs were recorded on a PDP 11/34 computer, with sampling rates of 50 kHz for *B. niger* and *G. petersii* and 100 kHz for *P. adspersus*.

Data analysis

All data were originally analysed using codes written in FORTRAN. For the present analyses, all data were re-analysed using IGOR Pro (WaveMetrics). The original code and resultant plots of data were used as reference.

Tuning curves. The best frequency was determined by finding the frequency with the lowest threshold stimulus (highest attenuation), which was set as 0 dB. Tuning curves were plotted as threshold stimulus, expressed as the dB attenuation required to evoke a threshold response at each frequency subtracted from the dB attenuation at the best frequency, *vs*. stimulus frequency in Hz. The width of tuning was quantified by dividing the best frequency by the bandwidth calculated as the difference between frequencies at which threshold is 10 dB. This empirical measure of tuning width based on treating Knollenorgans as bandpass filters was termed Q_{BP} to distinguish it from the fitted quality factor, Q, for a resonance filter described below.

Tuning curves were fit with the equation for a parallel resonance filter, as used to describe the electrical resonance of auditory hair cells (Crawford & Fettiplace, 1981), multiplied by the equation for a four-pole bandpass filter, which was required to capture the broader tuning observed in Knollenorgans. For fitting, the dB attenuation was converted back to amplitude (non-log scale).

The parallel resonance filter is a capacitor, C, in parallel with an inductor, L, and resistor, R, in series. The equation for parallel resonance is (eqn (1))

$$y_{\text{res}} = \frac{A_{\text{res}}}{F_0}\sqrt{\frac{Q^2 + \left(\frac{F_0}{F}\right)^2}{Q^2\left(\frac{F}{F_0} - \frac{F_0}{F}\right)^2 + 1}} \tag{1}$$

where F is frequency, F_0 is the resonant frequency, A_{res} is a scaling factor and Q is the quality factor that describes the sharpness of tuning, calculated as the dimensionless ratio of the resonant angular frequency, $1/\sqrt{LC}$, to the damping constant, R/L; higher Q values indicate sharper tuning and prolonged resonance (Crawford & Fettiplace, 1981).

The equation for a bandpass filter is (eqn (2))

$$y_{\text{BP}} = A_{\text{BP}}\sqrt{\frac{1}{1 + \left(\frac{F}{\text{HP}_c}\right)^4}} \times \sqrt{\frac{\left(\frac{F}{\text{LP}_c}\right)^4}{1 + \left(\frac{F}{\text{LP}_c}\right)^4}} \tag{2}$$

where F is frequency, HP_C is the corner frequency for the high-pass filter, LP_C is the corner frequency for the low-pass filter and A_{BP} is a scaling factor. Because the two equations were multiplied, the individual scaling factors were lumped into a single term.

Reverse correlation. Reverse correlations (spike-triggered reverse averages) were computed for each Knollenorgan by playing the tape recording backward at 1/8 speed (7.5 inches/s). The PDP 11/34 computer sampled 5.12 ms of noise (real time) following each spike trigger pulse, usually for 2016 spikes (minimum 672 spikes in the quietest unit). The samples were digitized at 20 μs/point by an AD-11K analogue to digital converter (12 bits), and the reverse correlation, $h(\tau)$, for the Gaussian white noise stimulus $x(t)$ was computed by averaging the noise segments preceding each spike, as (eqn (3))

$$h(\tau) = \frac{1}{N}\sum_{i=1}^{N} x(t_i - \tau) \tag{3}$$

where N is the number of spikes, t_i are the times when a spike occurs and τ is the lag from the spike

(ranging from 0 to 5.12 ms in 10 μs increments). If the Knollenorgan can be approximated as a linear filter, the reverse average should be proportional to the impulse response of the system (de Boer, 1968, 1969; de Boer & de Jongh, 1978). The amplitude of the reverse average is proportional to the magnitude of the noise stimulus that most effectively evokes spikes. The peak amplitudes varied across units, which may reflect biological variability across Knollenorgans, but likely also arose from differences in electrode location and other recording parameters. Because the relative, time-varying aspects of each impulse response, rather than the absolute magnitudes, were of interest, reverse averages were baseline-subtracted and normalized by the peak amplitude for display and analysis.

Comparisons of gain curves and tuning curves. Gain curves were computed from the spectral sensitivity curve of the fast Fourier transform (FFT) of the reverse averages. The maximal value of the amplitude spectrum was taken as the reference amplitude (a_{ref}), set at 0 dB, and the rest of the amplitude values (a) were converted to dB as $20\times\log(a/a_{ref})$. Gain curves were inverted and superimposed on tuning curves for comparison. Because points on the FFT were equidistant on a linear frequency scale and tuning curve points were equidistant on a log scale, the x-values of the two plots did not have a 1:1 correspondence. Therefore to estimate the correlation between the two curves the gain curve was first smoothed, and then points corresponding to the x-values of the tuning curve were calculated by linear interpolation. The interpolated gain curve points were plotted against the corresponding points of the smoothed tuning curve and were fitted linearly.

Convolution of reverse averages with arbitrary waveforms. For prediction of compound PSTHs the reverse average was linearly convolved with the noise stimulus used to generate PSTHs. The convolved waveform ('the convolution') and compound PSTH were cross-correlated, and the convolution was shifted by the time of maximal correlation. The shifted convolution was plotted against the compound PSTH and fitted with a third-order polynomial of the form $y = K_1x + K_2x^2 + K_3x^3$. The fit parameters K_1, K_2 and K_3 were used to scale the shifted convolution. The match between the scaled, shifted convolution and the compound PSTH was calculated as the variance accounted for, σ^2_{acctd}, given as (eqn (4))

$$\sigma^2_{acctd} = 1 - \frac{SSE_{PSTH-conv}}{\sigma^2_{PSTH}} \quad (4)$$

where $SSE_{PSTH\text{-}conv}$ is the sum of the squared errors from the differences between the compound PSTH and the scaled, shifted convolution, and σ^2_{PSTH} is the variance of the PSTH.

Results

Frequency ranges of electrical tuning of Knollenorgans

To measure the range of electrical tuning of Knollenorgans, spike-like receptor potentials (hereafter called 'spikes') evoked by electrical stimuli were recorded from Knollenorgans in immobilized fish. Recordings were made in three species, *B. niger*, *G. petersii, and P. adspersus*; data were obtained from 84 Knollenorgans (of 91 attempts). Most Knollenorgans fired in the absence of stimulation (73/83; no data stored from one unit). Spontaneous rates ranged from 0 to 84 spikes/s in all species, with one high-firing outlier per species. Excluding the outliers, the means ± SDs for spontaneous rates for *B niger*, *G. petersii,* and *P. adspersus* were 22 ± 23 spikes/s (N = 45/46), 21 ± 26 spikes/s (N = 19/20) and 34 ± 25 spikes/s (N = 16/17), and the outlier rates were 216, 321 and 216 spikes/s, respectively.

Application of sinusoidal electrical stimuli (100 ms) increased spike probability in all units. The filter properties of each unit were assessed by varying the intensity of each stimulus to find the lowest level (threshold) required to evoke a pre-set increase in firing above the spontaneous rate for each frequency, diagrammed in Fig. 1*A*. Threshold tuning curves were obtained by plotting threshold stimulus *vs.* stimulus frequency (Fig. 1*B*, Bass & Hopkins, 1984; Lyons-Warren et al., 2012). The best frequency was identified as the frequency that evoked a response at the lowest intensity level, which ranged from 5 to 250 nA extracellular stimulation across Knollenorgans (N = 84). As is evident from the fluctuations in the threshold values of the tuning curves, this measurement of best frequency is subject to some noise. By sampling more than 100 frequencies, however, this approach provides five- to sixfold greater resolution than comparable studies, facilitating estimates of best frequency to the nearest ∼10 Hz (exceptions noted below), as well as describing the filter characteristics away from the region of highest sensitivity. In the units for which tuning curves were successfully recorded more than once, the data were well replicated (Fig. 1*B*), suggesting that, to a first approximation, this approach provides a reliable assessment of frequency selectivity.

Figure 1*C* illustrates tracings of each species with the locations of recorded Knollenorgans. Units most clearly visible under the dissecting scope were located on dorsal surfaces and areas with dark pigment, including around the eye, over the operculum (between eye and gill) and along the back (Carlson et al., 2011). Broadly classifying best frequencies of units as low (<1.5 kHz),

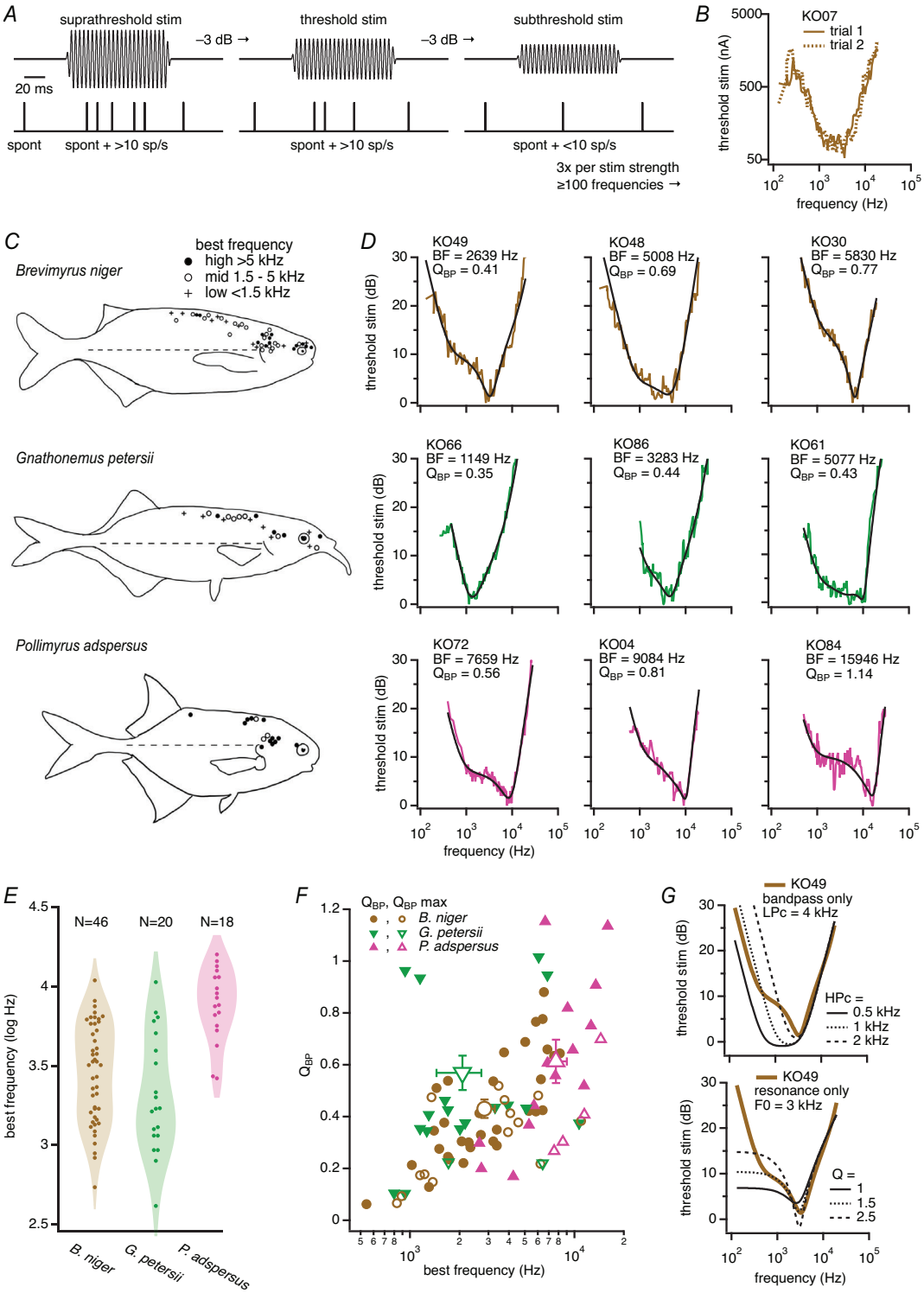

Figure 1. Tuning properties of Knollenorgans in three species of mormyrid electric fish
A, diagram of the experimental protocol. Sine wave stimuli (100 ms duration, 5 ms rise and fall) applied with different intensities (*top*) during spikes detected by a Schmitt trigger and recorded as binary output (*bottom*). Online spike counts compared firing during the stimulus with spontaneous firing (*spont*) occurring between stimuli. *Supra-threshold stim*: stimulus-associated firing >10 spikes/s (*sp/s*) above the spontaneous rate, as well as when stimulus intensity was decreased by 3 dB. *Threshold stim*: stimulus-associated firing >10 spikes/s above the spontaneous rate, but not when stimulus intensity was decreased by 3 dB. (See *Methods* for exceptions.) *Subthreshold stim*: stimulus-associated firing <10 spikes/s above the spontaneous rate. Three replications were done at each stimulus

strength. *B*, example tuning curves produced by the protocol in *A* for KO07. Threshold stimulus in nA is plotted against stimulus frequency in Hz. Two tuning curves are overlaid to illustrate replicability. Note that the frequency at which a threshold response is attained with the lowest stimulus intensity is set as 0 dB in all other tuning curves and analyses. *C*, tracings of *Brevimyrus niger* (*top*), *Gnathonemus petersii* (*middle*) and *Pollimyrus adspersus* (*bottom*). Locations of Knollenorgans from which recordings were made are marked with symbols indicating the tuning curve best frequency. Units are classed as high (>5 kHz, *filled circles*), mid (between 1.5 and 5 kHz, *open circles*) or low (<1.5 kHz, *crosses*). For high, mid, low *B. niger*: N = 13, 20, 10 (+1 in each category with no location recorded); *G. petersii*: N = 5, 7, 8; *P. adspersus*: N = 12, 3, 0 (+3 high-tuned units with no location recorded). *D*, (*top)* example tuning curves for three Knollenorgans (KO followed by unit number) from *B. niger* illustrating a range of best frequencies (BF) and tuning sharpness (Q_{BP}). Fits of the product of a resonance and bandpass filter are superimposed on each tuning curve (*black lines*). Fit parameters HP_C, LP_C, F_o and Q are as follows: KO49: 0.4 kHz, 17.4 kHz, 3.3 kHz, 1.5; KO48: 0.7 kHz, 8.0 kHz, 5.1 kHz, 0.9; KO30: 1.1 kHz, 16.5 kHz, 6.7 kHz, 2.2. *Middle*, as in top row for *G. petersii*. Fit parameters HP_C, LP_C, F_o and Q are as follows: KO66: 1.4 kHz, 7.7 kHz, 1.1 kHz, 0.9; KO86: 1.2 kHz, 18.6 kHz, 4.8 kHz, 1.2; KO61: 1.0 kHz, 4.8 kHz, 10.3 kHz, 2.4. *Bottom*, as in top row for *P. adspersus*. Fit parameters HP_C, LP_C, F_o and Q are as follows: KO72: 0.8 kHz, 11.0 kHz, 9.7 kHz, 1.3; KO04: 1.1 kHz, 6.5 kHz, 10.3 kHz, 2.5; KO84: 0.7 kHz, 12.7 kHz, 17.4 kHz, 2.1. *E*, violin plot showing the range of best frequencies for all units, N = 46, 20 and 18, as labelled. *F*, plot of Q_{BP} *vs*. best frequency for all Knollenorgans. *Closed symbols*, tuning width (Q_{BP}) measured as best frequency divided by bandwidth at 10 dB. *Open symbols*, for units in which the highest or lowest frequency tested was <10 dB, the extreme frequency was used to estimate the maximal Q_{BP}. *G*, illustration of tuning curve shapes predicted by pure bandpass filters (*top*) and pure electrical resonance (*bottom*), with a single parameter varied to show how filter shape changes. The bandpass filters all have a low-pass filter corner frequency LP_C of 4 kHz, and the high-pass filter corner frequency HP_C is varied (0.5 kHz, 1 kHz, 2 kHz, *black solid, dotted* and *dashed lines*), giving Q_{BP} values of 0.21, 0.29 and 0.41. The scaling factor A_{BP} was increased with HP_C (1000, 4000 and 16,000, respectively) to facilitate comparison of the low-frequency branch of the curves. The resonance filters all have a F_0 of 3 kHz, and the Q factor is varied (1, 1.5, 2.5, *black solid, dotted* and *dashed lines*). In both plots the fit to the data from KO49 from a combined resonance and bandpass filter (as shown in the leftmost panel in *B*) is superimposed for comparison (*brown lines*). All *y*-values have been converted to dB (with 0 dB equal to the threshold stimulation for the experimental data from KO49 as in *D*) and inverted to facilitate comparison to the tuning curves.

mid-range (1.5–5 kHz), and high (>5 kHz) revealed no overt tonotopic organization, although in *B. niger*, high-frequency units were highly represented around the eye, and low- and mid-frequency units predominated along the back. Nevertheless units tuned above 5 kHz were present in all species, particularly *P. adspersus*, in which low-frequency units were absent.

Sample tuning curves spanning a range of frequency sensitivities are shown for *B. niger*, *G. petersii,* and *P. adspersus* (Fig. 1*D*, *coloured lines*). Thresholds at each frequency are given relative to the lowest stimulus intensity level that evoked a response (0 dB), which occurs at the best frequency; 6 dB is thus a doubling of the stimulus intensity required to elicit a response. Most units showed 2- to 32-fold differences in sensitivity across the range of frequencies tested. The best frequencies spanned about 1 log unit in *B. niger* (range, 543–10,952 Hz, mean ± SD, 3580 ± 2390 Hz, $N = 46$) and *G. petersii* (range, 414–10,671 Hz, mean ± SD, 2970 ± 2710 Hz, $N = 20$), with *P. adspersus* covering a narrower window, biased to higher frequencies (range, 2639–15,946 Hz, mean ± SD, 8660 ± 3940 Hz, $N = 18$; Fig. 1*E*). In *P. adspersus* a second, narrow but prominent trough between 1000 and 3000 Hz was present in 8 of 18 tuning curves, as in KO84 (Fig. 1*D*, *bottom right*); whether this trough is real or artefactual is uncertain. Notably, this trough led to the classification of two Knollenorgans (KO01 and KO74) as having best frequencies <3 kHz, although both units also had high sensitivity in the high-frequency range (see below).

The breadth of tuning was assessed as Q_{BP}, calculated as the best frequency divided by the bandwidth at a threshold of 10 dB; larger values thus indicate narrower tuning or more selective filters. Unlike the sharp tuning of auditory hair cells, which have Q_{BP} values of 1–9 (Crawford & Fettiplace, 1980; Dallos, 1985), most values of Knollenorgans fell between 0.1 and 1.0 (Fig. 1*F*), with broader tuning at lower best frequencies.

As is evident in the plots of Fig. 1*D*, however, many tuning curves included inflexions absent from simple bandpass filters, which, on log axes, would always be concave upward or linear (Fig. 1*G*, *top*, *black lines*; Lyons-Warren et al., 2012). Nor did the curves have a shape characteristic of a sharply tuned electrical resonance, defined by the resonant frequency, F_0, and the quality factor, Q, that quantifies the sharpness of the filter; such curves would be concave-down on each side of the region of maximal sensitivity (Fig. 1*G*, *bottom*, *black lines*; Crawford & Fettiplace, 1981). Instead, many tuning curves resembled a bandpass filter at the extremes but included a region of higher sensitivity, evident as a dip in the threshold, that protruded from the bandpass-like waveform to produce an inflected or lobed curve.

Tuning curves were therefore fitted with the product of the equations for a resonance and a four-pole bandpass filter (Fig. 1*D*, *black lines*). Good fits, which converged and did not obviously deviate from the data by eye, were obtained in 68 of 84 tuning curves (81%); most remaining curves had best frequencies too close to one extreme

of the tested range for a good estimate of parameters, or appeared to have multiple troughs, which gave the tuning curves a W-shape. In the good fits from *B. niger* (N = 38/46), *G. petersii* (N = 16/20), and *P. adspersus* (N = 14/18), respectively, the resonant frequencies, F_0, were 5.9 ± 2.4 kHz, 5.1 ± 3.8 kHz, and 12.6 ± 4.1 kHz, and the quality factors, Q, were 0.90 ± 0.56, 1.49 ± 1.34, and 1.30 ± 0.50 (mean ± SD). The corner frequencies of the high-pass component (HP_C) were, respectively, 0.9 ± 0.7 kHz, 1.4 ± 0.7 kHz, and 1.2 ± 0.7 kHz, and, for the low-pass component (LP_C) 16.0 ± 10.9 kHz, 12.2 ± 9.2 kHz, and 17.1 ± 11.4 kHz (mean ± SD). Superimposing the good fit obtained by this method for the tuning curve from KO49 on the pure bandpass and pure resonance filters in Fig. 1*G* emphasizes that the experimental data deviated from the simple U- or trapezoidal shape of bandpass filters, even with varying corner frequencies, as well as from the arched V-shape of the resonance filter, even with varying Q values. The results are consistent with the idea that the tuning of Knollenorgans is shaped by factors that behave like an electrical resonance, which can extend well above 5 kHz.

Relation of Knollenorgan tuning properties to the EOD

Knollenorgans are considered communication sensors, because they respond to the EODs of conspecifics, whereas self-generated EODs are cancelled by corollary discharge inhibition (Bass & Hopkins, 1984; Bell & Grant, 1989; Hopkins & Bass, 1981; Zipser & Bennett, 1976). Therefore, we directly examined how the tuning curves measured here, which provide an indication of the range of frequencies that Knollenorgans detect, relate to species-specific EODs. EODs were recorded from *B. niger* and *G. petersii* (Fig. 2*A*, *top* and *middle*), as well as *P. adspersus*, in which the EOD is sexually dimorphic (Crawford & Huang, 1999; Fig. 2*A*, *bottom*). All tuning curves from each species were inverted and superimposed on the power spectra of the corresponding EOD, which illustrate the frequencies present in each discharge (Fig. 2*B*). Two example tuning curves are highlighted for each species to illustrate that most individual tuning curves are narrower than the power spectrum. The set of Knollenorgans recorded, however, tile the full range of frequencies present in the EODs; Knollenorgans of *B. niger* have additional sensitivity into lower-frequency ranges. Notably in *P. adspersus* the high frequencies represented in the tuning curves extend across the correspondingly high frequencies in the EOD power spectra, which reach a peak at 9240 Hz (male) and 12,320 Hz (female), as compared to 5859 Hz for *B. niger* and 4395 Hz for *G. petersii*. Knollenorgans in all three species tested thus exhibit sensitivity suitable for detecting species-specific communication signals.

Impulse responses estimated from spike-triggered reverse averages of noise stimuli

The tuning curves of the Knollenorgans raise the question of the extent to which the filtering properties of these electroreceptors are linear. Such linearity has previously been probed and, to a first approximation, supported in

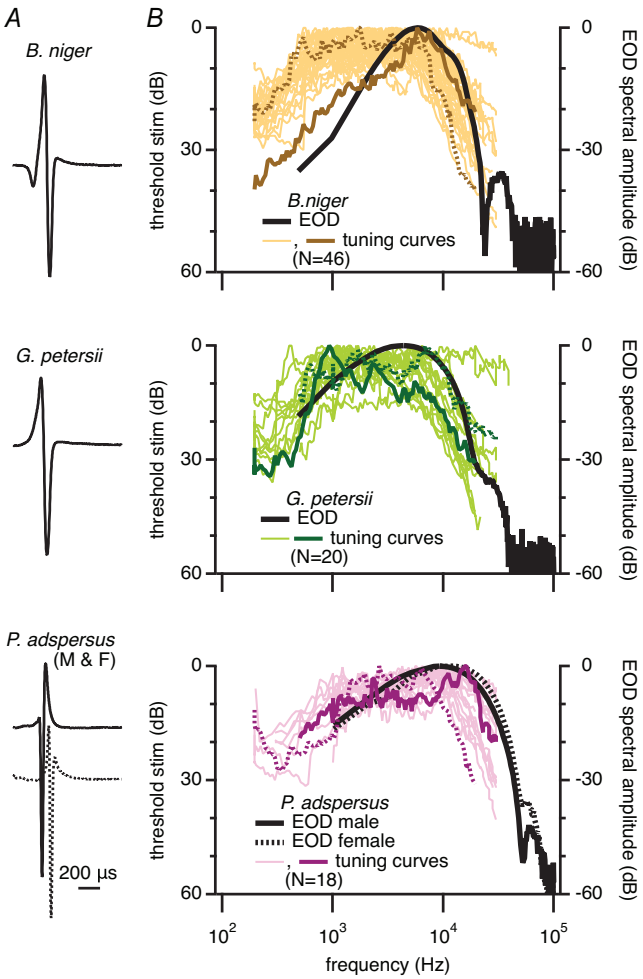

Figure 2. Relation of Knollenorgan tuning curves to electric organ discharge (EOD) power spectra
A, EODs of *Brevimyrus niger* (*top*), *Gnathonemus petersii* (*middle*), *Pollimyrus adspersus* (*bottom*; male, *continuous line*, female, *dotted line*). Time scale pertains to all panels. *B*, power spectra, plotted as spectral amplitude *vs*. frequency, from Fourier transforms of the EODs in *A*, with all tuning curves for each species (*top, middle, bottom, N* = 46, *N* = 20, *N* = 18) inverted and superimposed. Two curves are highlighted in each panel to facilitate comparison: *B. niger*, KO30 (*solid*) and KO42 (*dotted*); *G. petersii*, KO67 (*solid*) and KO91 (*dotted*); *P. adspersus*, KO84 (*solid*) and KO01(*dotted*). Note (inverted) W-shape of KO67 and low-frequency troughs in both KO01 (which defines the best frequency) and KO84.

auditory nerve fibres through the technique of reverse correlation, which makes use of the characteristic of sensory systems to transform an analog input into an output of a series of impulses, i.e. action potentials (de Boer, 1968, 1969; de Boer & de Jongh, 1978; see also Bialek & Rieke, 1992). On the assumption of linearity, the impulse response of the system can be calculated by evoking spikes by a broadband noise stimulus and then averaging the noise preceding each spike. This spike-triggered reverse average (hereafter simply 'reverse average') is a measure of the impulse response of the system. As such its gain curve, obtained as the power spectrum from the Fourier transform, represents the filter properties of the system. Therefore, if the system is indeed linear, the gain curve should match the tuning curve obtained by single-frequency sinusoidal stimuli. This approach has been used successfully to describe tuning curves of inner hair cells (Dallos, 1985).

Here we applied the technique of reverse correlation to Knollenorgans. Each Knollenorgan was stimulated with 30 s of pseudo-random Gaussian white noise, and spikes were recorded. By playing the recording backward and triggering to the time of each spike, we calculated the mean of all noise segments (duration, 5.12 ms) preceding each spike, which generated the reverse average, schematized in Fig. 3*A*. As expected, the waveforms of reverse averages varied across Knollenorgans (Fig. 3*B*). The gain curves were computed from the Fourier transforms and inverted to conform to tuning curve plotting conventions (with 0 dB indicating maximal power or minimal threshold). As shown in Fig 3*C* (*top*) for *B. niger,* overlaying the tuning curves of the corresponding Knollenorgan revealed good matches between each tuning curve elicited by sinusoids and inverted gain curve from the impulse response computed from white noise stimuli. Assessing the overlap was complicated by the fact that the *x*-values of the two curves were different, because successive points on the tuning curve were equidistant on a log scale, but successive points on the gain curve increment linearly, owing to the FFT calculation. Therefore to evaluate the quality of the match between the curves we smoothed both curves and then interpolated to generate a one-to-one correspondence between points on the gain and tuning curves (see *Methods*). The interpolated, smoothed gain curve was plotted against the smoothed tuning curve, and the data were fitted with a straight line. Figure 3*C* (*bottom*) shows these plots for three example Knollenorgans, in which correlation coefficients (R) were 0.95, 0.84 and 0.95. When the same analysis was performed for all 36 Knollenorgans for which both tuning and gain curves were measured, 78% (28/36) had correlations above 0.5 (Fig. 3*D*).

When the same analyses were performed for *G. petersii* (Fig. 3*E* and *F*), the tuning curves and inverted gain curves again overlapped, with 83% (15/18) Knollenorgans having R-values above 0.5. Similarly, in *P. adspersus* (Fig. 3*G* and *H*), 87.5% (7/8) of the R-values exceeded 0.5. Of the 12 of 63 units across species that were poorly correlated, eight of them (KO16, KO21, KO22, KO44, KO47, KO61, KO84, KO86) had high sensitivity to frequencies above the filter cut-off of the noise stimulus, which was 10 kHz for *B. niger* and *G. petersii* and 20 kHz for *P. adspersus*, which necessarily limited the accuracy of the reverse average. The mismatches of the other four (KO23, KO24, KO31, KO88) may reflect genuine non-linearities but may also have resulted simply from drift in recording conditions between acquisition of the tuning curve and application of the noise stimuli. The strength of the correlations in most Knollenorgans supports the idea that, even though the ionic mechanisms that support the transduction from external electrical stimulus to neural signal may involve voltage-gated conductances or other non-linear components, the first stage of processing can indeed be approximated as a linear filter.

Nevertheless the next stages of processing include non-linearities. Specifically, Knollenorgans only generate spikes to the outside-positive phase of the electrical signal (Bennett, 1965; Hopkins & Bass, 1981), introducing a second stage, of rectification. Additionally spikes are not generated instantaneously but occur with a latency, introducing a third stage, of a lag. Finally the probability of firing, which is governed by spike threshold, varies non-linearly with respect to voltage, introducing a fourth stage, of supralinear scaling; in mammalian neurons in which it has been measured directly and modelled this scaling follows a power-law relationship (Anderson et al., 2000; Hansel & van Vreeswijk, 2002; Troyer et al., 2002). To investigate the extent to which this simple four-step model adequately captures the transformations from the sensory stimulus to the spike output of electroreceptors, we stimulated Knollenorgans with arbitrary electrical waveforms, recorded their responses, and tested whether their spiking could be predicted from the previously recorded reverse average passed through the additional stages of processing.

The approach is illustrated in Fig. 4 for one Knollenorgan, KO07, from *B. niger*. After the reverse average was recorded, we recorded spikes evoked by a 10-ms 'noise stimulus', which consisted of a step calibration pulse and a segment of Gaussian white noise, here filtered at 10 kHz. The noise stimulus was repeated 2000 times, and a PSTH with 0.2 ms bins was constructed (Fig. 4*A*, 'upright' noise, *black*; PSTH, *light blue*). Consistent with rectification spikes were fired only on the positive phase of the noise signal. Therefore we switched the polarity of the noise signal and repeated the stimuli for another 2000 sweeps, from which a second PSTH was constructed and plotted as negative (Fig. 4*A*, 'inverted' noise, *purple*; PSTH, *lilac*); note that the inverse waveform is what is expected to be detected

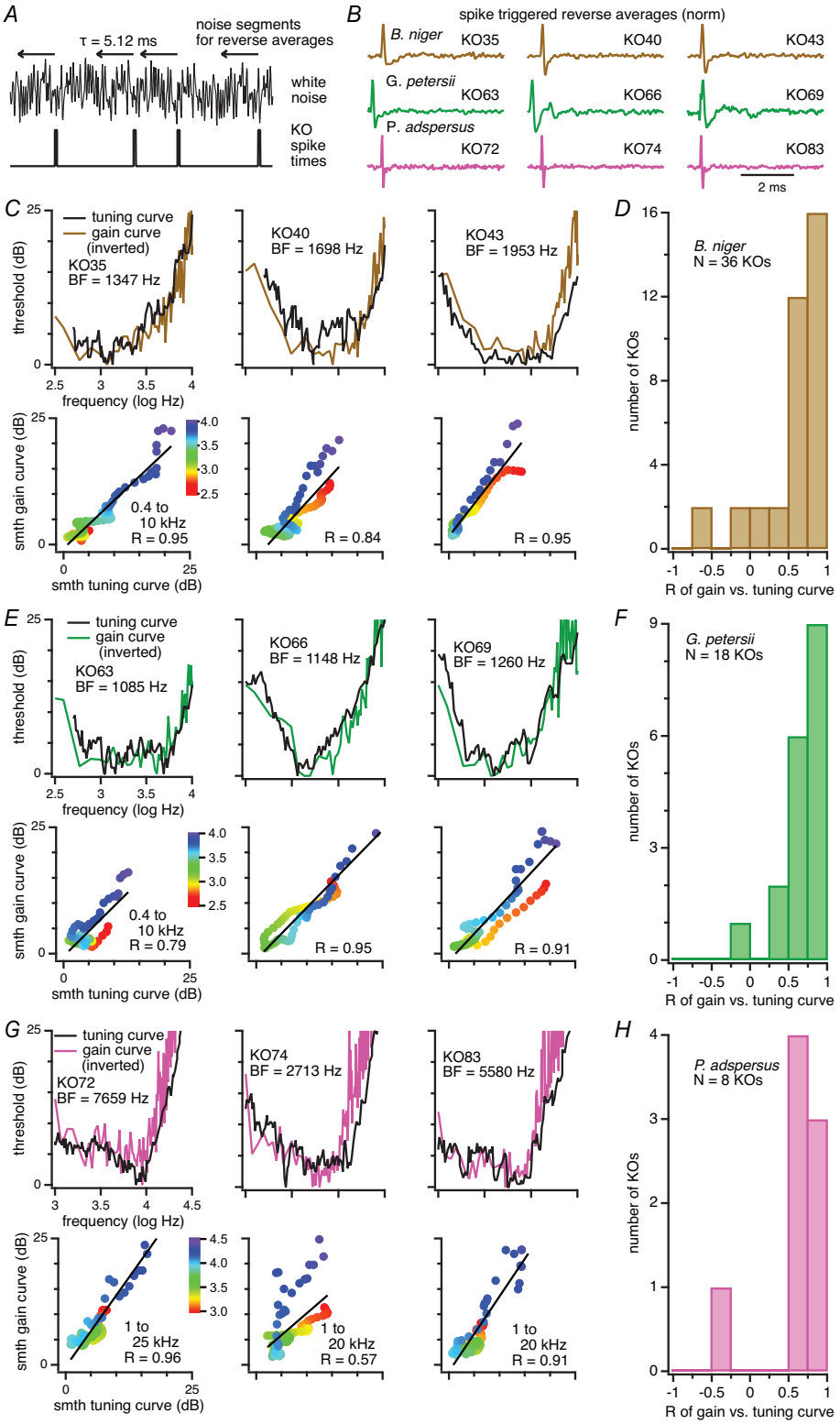

Figure 3. Correlations of tuning curves and gain curves of spike-triggered reverse averages
A, method of obtaining spike-triggered reverse averages. Schematics of white noise stimulus (*top*) and spike times detected by a Schmitt trigger and recorded as binary output (*bottom*). *Arrows* indicate the 5.12 ms noise segments preceding each spike, from which the reverse average was generated. *B*, example reverse averages, normalized to the peak amplitude, for three Knollenorgans (KO followed by unit number) from each species, as labelled. *C*, *upper panels*, overlay of tuning curves and inverted gain curves for the Knollenorgans of *Brevimyrus niger* illustrated in

B. 0 dB indicates the frequency with the lowest threshold for the tuning curve and the highest spectral amplitude for the gain curve. *Lower panels*, scatter plot of interpolated and smoothed (*smth*) gain curve *vs*. the smoothed (*smth*) tuning curve. The colour scale bar represents frequency in log Hz. *Continuous line*, linear fit to the data. The correlation coefficient R is indicated on each plot. *D*, distribution of correlation coefficients from linear fits, as in *C*, for all 36 Knollenorgans. *E*, as in *C*, for *Gnathonemus petersii*. *F*, as in *D*, for *G. petersii*. *N* = 18 Knollenorgans. *G*, as in *C*, for *Pollimyrus adspersus*. *H*, as in *D*, for *P. adspersus*. *N* = 8 Knollenorgans.

by Knollenorgans on the side of the fish opposite to the stimulus source. Summing the positive-going and negative-going histograms produced the 'compound PSTH', which served to eliminate the relatively small amount of spontaneous firing and capture the full response to the noise stimulus (Fig. 4*B*).

We next tested whether this response could be predicted from the reverse average by considering the four stages above. For a linear filter, the output to any arbitrary input is given by the convolution of that input with the impulse response. We therefore first convolved the noise stimulus with the reverse average (Fig. 4*C*). Second, the latency to spiking was accounted for by cross-correlating the convolution with the compound PSTH. The cross-correlation had a clearly identifiable peak, which in the case of KO07 was at 400 μs (Fig. 4*D*). Third, the values of the convolution, shifted by 400 μs, were plotted against the values of the compound PSTH. This plot revealed that the prediction from the time-shifted convolution and the experimental data was indeed systematically related, and the points could be reasonably well fit with a third-order polynomial, consistent with a supralinear relation between spike probability and stimulus magnitude (Fig. 4*E*). Fourth, the time-shifted convolution was scaled by the polynomial and superimposed on the compound PSTH (Fig. 4*F*). The goodness of fit was quantified as the variance accounted for (σ^2_{acctd}, computed from the ratio of the sum of the squared errors between the prediction and the data to the variance of the data, subtracted from 1). In the case of KO07 the prediction accounted for 84% of the variance in the data.

In five Knollenorgans, all from *B. niger*, we were able to repeat this analysis under nine stimulus conditions (Fig. 5*A*, *top panels*), which varied in the amplitude of the noise (high, mid, and low amplitude, spanning a range of 5–6 dB) and in the high-frequency cut-off of the noise (10-, 5-, and 2.5 kHz; power spectra in Fig. 5*B*). The overlay of the PSTHs and the predictions from the reverse average for all conditions is shown for KO27 (Fig. 5*A* *bottom*), which had the best frequency of 3367 Hz. The prediction of the timing of increases and decreases in spike probability is remarkably accurate in all conditions. Given that the bin widths are 0.02 ms, these data indicate that environmental electrical signals are transduced and transmitted with an extremely high temporal fidelity.

The deviations between predicted and actual responses resulted from mismatches in magnitude rather than timing, in that the highest spike probabilities were consistently underestimated. Furthermore, these deviations were largest with the stimuli of highest intensity. Indeed, for KO27, the total variance accounted for ranged from 40% for the high-amplitude 10 kHz noise to about 80% for the low-amplitude stimuli of 5 and 2.5 kHz noise. A similar pattern of the prediction from the reverse average accounting for >50% of the variance was present in four of the five Knollenorgans (Fig. 5*C*; mean ± SD for all five Knollenorgans, 10, 5, 2.5 kHz, high amplitude, σ^2_{acctd}, 47 ± 11%, 60 ± 12%, 63 ± 19%; low amplitude, σ^2_{acctd}, 63 ± 19%, 71 ± 19%, 72 ± 19%). The exception was KO22 (best frequency 831 Hz), in which the prediction was relatively poor regardless of the noise characteristics. A different type of exception was KO15 (best frequency 6404 Hz), which was the only unit that lacked consistently greater accuracy of the prediction for the low-intensity stimuli, but this unit had an unusually weak response to the low-amplitude 2.5 kHz noise, resulting in a noisy PSTH for that condition. Overall the observation that the analysis accounted for 50% of the variance for most of the nine conditions in all but one Knollenorgan provides support for the model of linear filtering followed by spike threshold non-linearity.

Similar experiments were conducted with fewer noise frequencies and strengths in 6 additional Knollenorgans from *B. niger*, 2 from *G. petersii*, and 7 from *P. adspersus*, for a total of 19 Knollenorgans tested. In all cases, the reverse average was convolved with the noise stimulus, shifted by the lag from the peak of the cross-correlation, and scaled, and then the predicted response was compared to the measured PSTH. Across units, the lag ranged from 400 to 500 μs (mean ± SD, 470 ± 25 μs). Although these values are not strictly comparable across units because of the arbitrary relation between spike initiation and Schmitt trigger level, with higher levels estimating longer lags, they nevertheless indicate that the latency from stimulus to threshold is exceedingly short.

In 18 of the 19 Knollenorgans tested, the prediction accounted for more than 50% of the variance (69 ± 9%, $N = 18$) across the full range of best frequencies recorded (range: *G. petersii* KO68 at 403 Hz to *P. adspersus* KO84 at 15 625 Hz, Fig. 6*A*). The one unit with <50% variance accounted for (*P. adspersus* KO80, best frequency 6853 Hz) was unusually sensitive, firing 20% more spikes (Z-score = 5.6) during the 30 s noise stimulus than the other Knollenorgans from the same species. Examination of the PSTH suggests that it may have been firing in bursts.

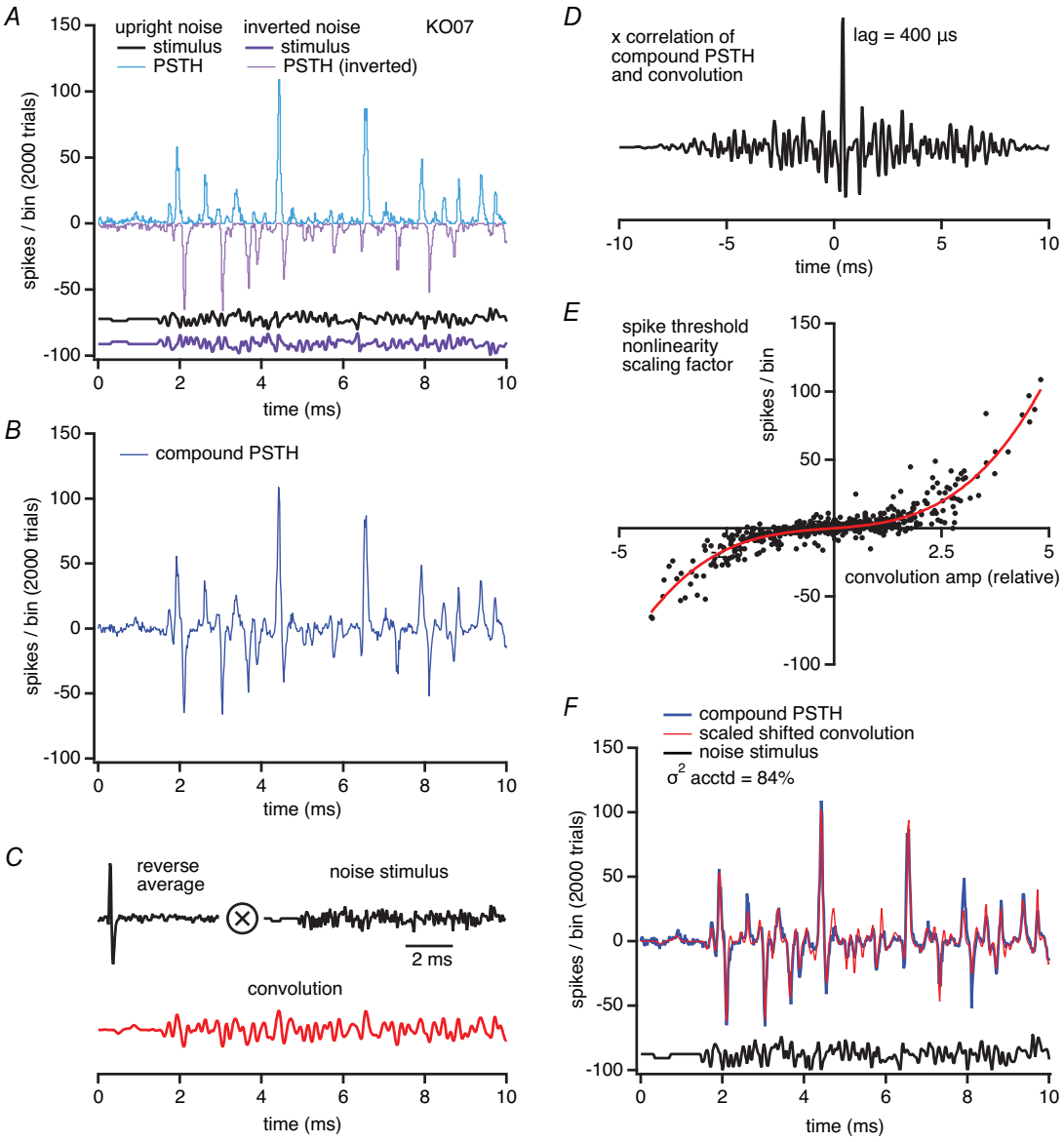

Figure 4. Predicting Knollenorgan spike responses to arbitrary stimuli from reverse averages
A, example of 10 ms noise stimulus (filtered at 10 kHz; upright, *black*; inverted, *purple*) and the corresponding peristimulus time histograms (PSTHs) (bin width 20 µs) resulting from 2000 stimulus repetitions (response to upright noise, *light blue*, 21,277 total spikes; response to inverted noise, *lilac*, plotted as negative, 20,710 spikes). The calibration step in the noise stimulus is 0.25 nA, and the maximal noise deflection is about 4 nA. Recordings in all panels are from KO07, from *Brevimyrus niger*. *B*, compound PSTH from summing the upright and inverted (negative) PSTHs in *A*. *C*, the reverse average (*top left*) and noise stimulus (*top right*) are convolved to give the predicted output of a linear filter (*red*). *D*, cross-correlation of the compound PSTH and the convolution, with peak at 400 µs. *E*, estimation of spike threshold non-linearity scaling function. The bin values from the compound PSTH in *B* (*black dots*) are plotted against the convolution from *C*, shifted by the lag computed in *D*. The *x*-units are relative amplitude, as they result from convolving the noise (in nA) with the reverse average that is normalized to 1. The data are fitted (*red line*) with a third-order polynomial, $y = K_1x+K_2x^2+K_3x^3$, with coefficients $K_1 = 2.369$, $K_2 = 0.331$ and $K_3 = 0.747$. *F*, the lag-shifted convolution scaled according to the polynomial fit (*red*), superimposed on the compound histogram (*blue*). The goodness of fit is taken from the variance accounted for (σ^2_{acctd}), defined in the text.

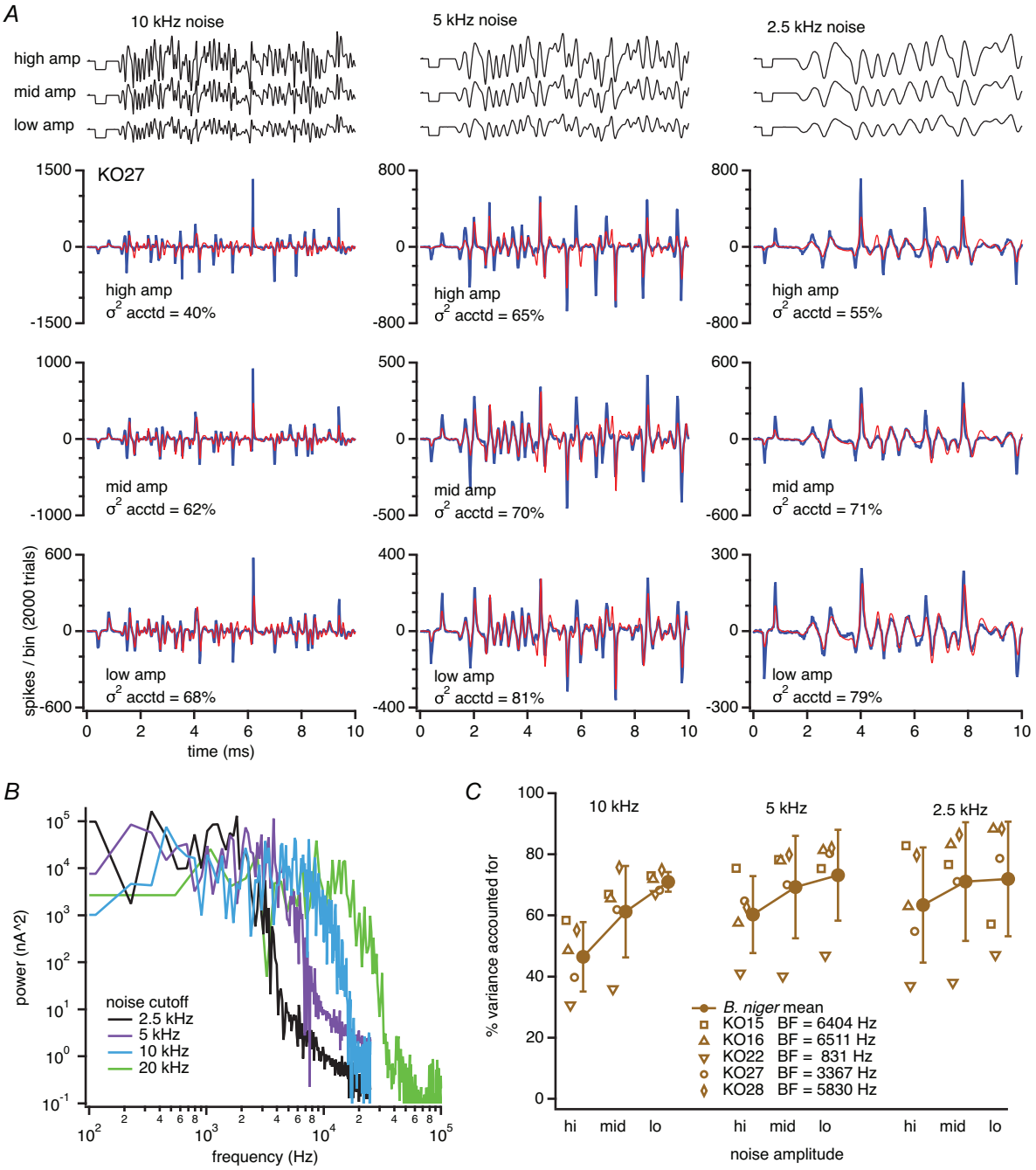

Figure 5. Reverse average predictions of PSTHs across different frequencies and intensities of stimuli
A, plots of sample compound peristimulus time histograms (PSTHs) (*blue*) and responses predicted by convolution of reverse averages with noise stimuli (*red*) from KO27 (*Brevimyrus niger*), for nine conditions. Noise stimuli (*black*) are shown above the PSTH plots. Intensity levels *high*, *mid*, and *low* (corresponding to the *top, middle,* and *bottom* PSTH plots, respectively) each differ by 3 dB, so that *high* is twice the amplitude of *low*. Cut-off frequencies are 10, 5, and 2.5 kHz (corresponding to the *left, middle,* and *right* plots respectively). Calibration signal is 2.5 nA in each noise stimulus. The variance accounted for is given on each panel as σ^2_{acctd}. *B*, power spectra of noise stimuli with 2.5, 5, 10, and 20 kHz filter cut-off frequencies as labelled. The 20 kHz stimulus was used only with *Pollimyrus adspersus*. *C*, summary data of variance accounted for by the reverse average prediction of PSTHs for the six Knollenorgans (all *B. niger*) for which a complete set of three intensities at three frequencies were obtained. Note that deviations were greatest with high-intensity noise, usually owing to more spikes than predicted by the portions of the stimulus that were most effective at producing spikes (as in top row in *A*).

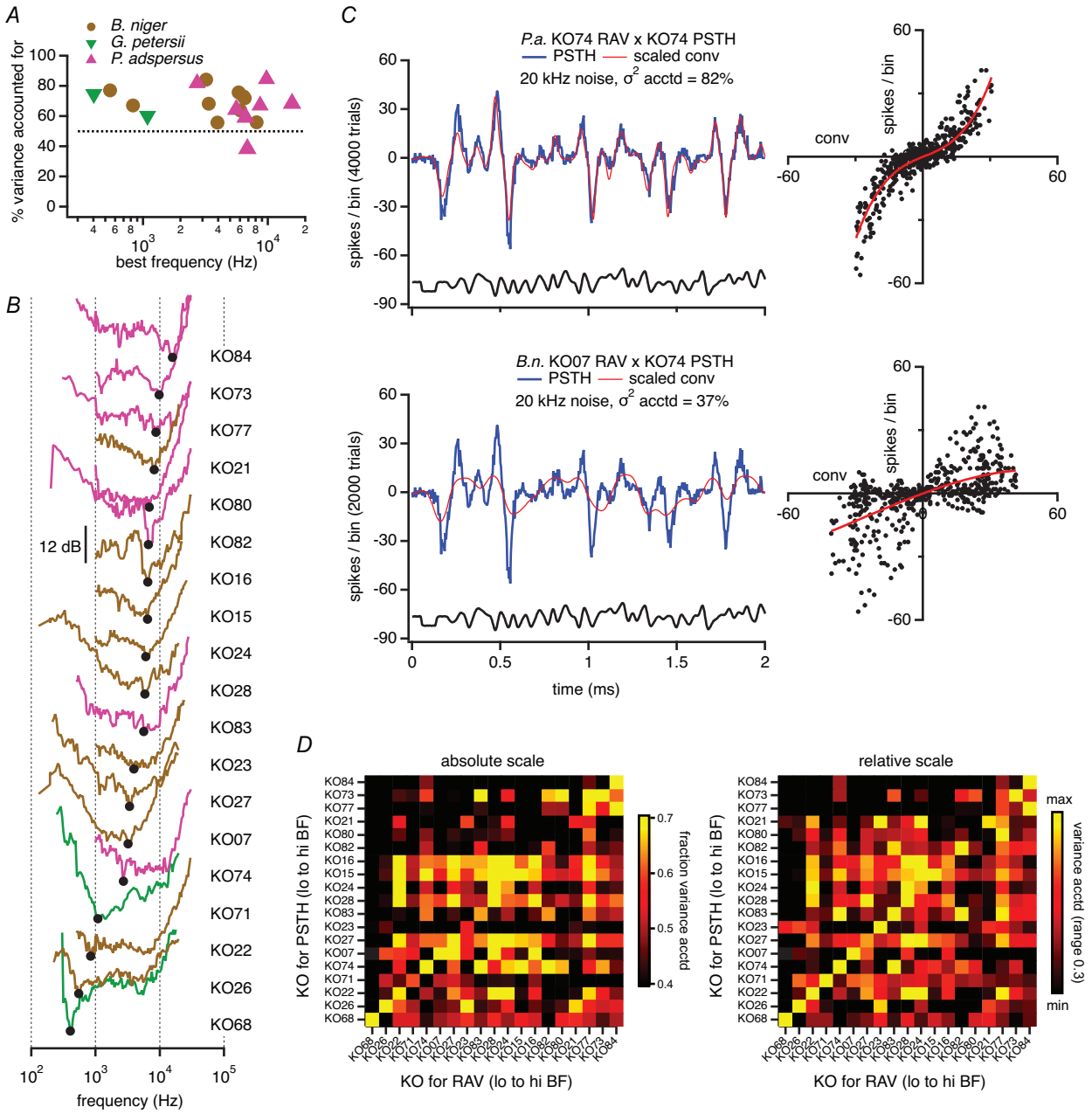

Figure 6. Efficacy and specificity of predictions of peristimulus time histograms (PSTHs) from reverse averages for all species

A, cross-species summary of variance accounted for in all 19 KOs for which convolution experiments were done, plotted against best frequency. Data are shown for 10 kHz noise stimuli for *Brevimyrus niger* (except 5 kHz for KO26, which for unknown reasons produced few spikes to the 10 kHz stimulus) and *Gnathonemus petersii* and 20 kHz for *Pollimyrus adspersus*. *Dotted line*, 50%. *B*, tuning curves of all Knollenorgans in *A*, ordered from the lowest best frequency (*bottom*) to the highest best frequency (*top*), offset by 12 dB between each curve. The specific units are labelled at right, aligned with the *black circle* that labels the best frequency of each curve. *B. niger*, *brown*, *G. petersii*, *green,* and *P. adspersus*, *pink*. *Dotted black lines* indicate 100, 1000, 10,000, and 100,000 Hz. *C*, *top left*, the 20 kHz noise stimulus (*black*, calibration step 2.5 nA), compound PSTH of KO74 (*blue*), and predicted response from the reverse average of KO74 (*red*). Variance accounted for, σ^2_{acctd}, 82%. *Top right*, plot of compound PSTH (*black dots*) *vs*. the lag-shifted convolution for computation of the spike threshold non-linearity scaling factor. *Bottom left*, as above, but with the response of KO74 predicted by the reverse average of KO07 (*red*). Variance accounted for, σ^2_{acctd}, 37%. *Bottom right*, as above, with the KO07 reverse average mismatched to the KO74 PSTH. *D*, *left*, heat map of the absolute fraction of σ^2_{acctd} with the PSTH of each Knollenorgan (*y*-axis) predicted by each reverse average (*x*-axis). Units are sorted from low to high best frequency (values plotted in *A*, full curves plotted in *B*). *Right*, heat map as at left, but with relative fraction of σ^2_{acctd}, so that the maximal σ^2_{acctd} in each

case is brightest, and colours shift to the darkest over a scale of 0.3. Note the bright diagonal, indicating the specificity of each reverse average for predicting the spike response of its own Knollenorgan.

It is possible that such hyper-responsiveness is reflective of another level of non-linearities in some Knollenorgans not accounted for in the present model, but this phenomenon was too rare in the dataset to study further.

The high correlation in most units between the responses predicted from the convolution and the PSTH, however, raises the question of the extent to which Knollenorgans in fact generate distinct responses, especially given the broad tuning of most units. Plotting all tuning curves of the Knollenorgans subject to this analysis and ordering them by nominal best frequency suggest that filtering is defined by more than this single parameter, because of the complex shapes that vary in both the width and range of tuning (Fig. 6*B*). Of particular interest is whether the sensitivities to high frequencies evident in some tuning curves, e.g. of *P. adspersus*, permit effective transmission of high-frequency components of the signal. As an example, the tuning curves of KO07 (*B. niger*) and KO74 (*P. adspersus*) are next to each other in the ranking by best frequency, largely owing to the low-frequency notch in the curve of KO74, which places its best frequency at 2713 Hz. Its low-threshold region extends well above 10 kHz, however, unlike KO07, in which the sensitivity drops 10-fold by 10 kHz. We therefore tested how well the PSTHs of each unit could be predicted by the filter properties of each of the other Knollenorgans. Like the other units from *P. adspersus,* KO74 was stimulated with noise segments filtered at 20 kHz. The convolution of the reverse average of KO74 with the noise was highly effective at predicting the experimental PSTH, accounting for 82% of the variance (Fig. 6*C*, *top*). In contrast, when the reverse average of KO07 was convolved with the 20 kHz noise segment, the prediction gave a poor approximation of the response of KO74, accounting for only 37% of the variance (Fig. 6*C*, *bottom*). The mismatch is not a consequence of inherent noisiness or other problems in the reverse average of KO07, however, since it successfully accounted for 84% of the variance of the response of KO07, as shown in Fig. 4. Instead the deviations are largely a result of a blunting of the temporal precision by the filtering properties of the lower-tuned Knollenorgan.

This cross-convolution analysis was repeated for all 361 pairs of the 19 Knollenorgans tested, and, for each pair, the variance accounted for was plotted as a heat map to illustrate the efficacy of each reverse average (Fig. 6*D*, *left*). Because the maximal variance accounted for ranged across units from 59% to 84%, however, this absolute depiction obscures the relative efficacy of the reverse averages. This relationship is better shown by linearly shifting the heatmap scale to set the peak variance accounted for (for each PSTH, by any reverse average) as the maximum for each Knollenorgan (Fig. 6*D*, *right*). The bright diagonal of this plot shows that, with the exception described above of KO80, each unit's own reverse average was a better predictor for that Knollenorgan's PSTH than 97% ± 5% of the other reverse averages of the other 18 units. These results demonstrate that the filter properties even of broadly tuned electroreceptors appreciably determine spike patterns, producing a distinct array of responses to a common input. Moreover they show that high-frequency tuned receptors indeed transduce and transmit responses to high-frequency components of electrical signals, providing evidence for effective coding by electrical tuning into the kilohertz range.

Discussion

These experiments demonstrate that Knollenorgans of mormyrid electric fish can detect frequencies of electrical stimuli well into the kilohertz range, with best frequencies exceeding 10 kHz in some species. Moreover, the high-frequency responsiveness of Knollenorgans reported here appears physiologically relevant: first, the three species of mormyrid fish tested here, which produce EODs with different spectral characteristics, have Knollenorgans with distinct tuning ranges that cover the frequencies present in the species-specific EOD, consistent with an adaptation to detect conspecific discharges. Second, the fluctuations in high-frequency noise stimuli up to 20 kHz are transduced into spikes with extraordinarily high temporal fidelity, as appropriate for relaying timing information relevant to social communication to higher brain centres. Third, distinct Knollenorgans on the same fish filter signals differentially, as is characteristic of sensory systems that peripherally decompose biologically relevant signals for central neural computations. Given that both the external signals and the neural responses are electrical, it appears highly likely that the sensory transduction process of Knollenorgans is largely electrical. These results therefore provide evidence that these electroreceptors must have mechanisms of electrical tuning that operate over a far greater range than in mechanosensitive hair cells, in which electrical resonance extends only to ∼2 kHz.

Comparison of tuning properties of tuberous electroreceptors

The frequency sensitivity of tuberous receptors, generally assessed by afferent nerve recordings, has been measured

in both mormyrid and gymnotid electric fish, in which EODs can be either pulse-like or wave-like. In the wave-discharging gymnotiforms *Sternopygus macrurus, Eigenmannia virescens,* and *Apteronotus albifrons*, tuberous receptors are tuned to 50–150, 250–500, and 800–1200 Hz, respectively; in each case, the maximal responsiveness is matched to the fish's own EOD spectra (Hopkins, 1976). Similar recordings from the pulse-discharging gymnotid *Gymnotus carapo* reveal tuning curves with best frequencies up to 2 kHz (Watson & Bastian, 1979), and multiple *Hypopomus* (*Brachyhypopomus*) species are tuned to the 1–2 kHz range (McKibben et al., 1993).

Similarly, the wave mormyroid, *Gymnarchus niloticus*, ancestor to Mormyridae, has Type S and Type O tuberous receptors tuned to 200–400 Hz, the frequency of the EOD waveform (Bullock et al., 1975). In the pulse mormyrids *P. batesii* and *Brienomyrus brachyistius*, in which EOD spectral frequencies extend higher, Knollenorgans again match the species-typical EOD spectrum, ranging from about 0.5–4 kHz (Bass & Hopkins, 1984; Hopkins, 1981; Hopkins & Bass, 1981; Lyons-Warren et al., 2012). Additionally, in pulse mormyrids with sex differences in EODs Knollenorgans are tuned to match these frequencies, and specimens treated with androgens show shifts of EOD spectra and Knollenorgan tuning to lower (male-like) frequencies, unless the fish's own EOD is electrically silenced (Bass & Hopkins, 1984).

The present work was motivated by the inference that EOD spectra may serve as a proxy for frequency sensitivity range of tuberous electroreceptors. Consistent with this idea, comparisons of best-frequency distributions in *B. niger*, *G. petersii* and *P. adspersus* confirm that the range of Knollenorgan tuning encompasses the frequencies in the conspecific EODs. Most striking, however, is that the present experiments greatly extend the range of best frequencies reported. For example in *P. adspersus*, which has a maximal EOD near 10 kHz, it is the rule rather than the exception to find the lowest response thresholds at frequencies >5 kHz, and in half the units tested best frequencies ranged from 8 to 16 kHz.

In all three species studied here, the physical distribution of Knollenorgans is broad, with units on the head, operculum and back. Such dispersion has been shown to be predictive of evolutionary diversification of the exterolateral nucleus of the midbrain in a manner that facilitates discrimination of EODs (Carlson et al., 2011). Unlike in *P. batesii* and *B. brachyistius*, however, in which Knollenorgans tuned to lower frequencies (<1 kHz) cluster dorsal to the operculum, and higher frequency units are scattered more broadly (Bass & Hopkins, 1984), no clear tonotopic organization was evident in these species. Although this result may reflect a true absence of tonotopy, it may be simply attributable to the limited sample size.

Transmission of temporal information by Knollenorgans in electric communication

The high-frequency sensitivity of Knollenorgans is associated with high precise temporal processing, which distinguishes these electroreceptors from ampullary organs and mormyromasts. Ampullary organs, present even in non-electric fish, respond to weak bioelectric fields produced by other aquatic organisms and are used in passive electrolocation. Accordingly, they are sensitive to slow modulations of 1–10 Hz (Bell, 1989; Crampton, 2019; Engelmann et al., 2010; Hopkins, 1976). Mormyromasts are used for active electrolocation, detecting objects by the distortions they produce in the fish's own EOD (Bell, 1989; Bennett, 1965). They, too, are broadly responsive to relatively low-frequency stimuli (0.05–1 kHz) and have 10–100-fold higher thresholds than Knollenorgans (Bass & Hopkins, 1984; Bell, 1990; Carlson et al., 2000; Hopkins, 1981; Hopkins & Bass, 1981; Lyons-Warren et al., 2012). In fact mormyromasts and their afferents are also strongly sensitive to intensity, with spike rates as well as spike latencies graded with stimulus strength (Bell, 1990). These changes in spike timing with stimulus strength are consistent with the idea that precise temporal information is not transmitted through these pathways.

In contrast, Knollenorgans faithfully transmit the temporal components of electrical signals, the feature that enables their responsiveness to the EODs of conspecifics (Bass & Hopkins, 1984; Hopkins, 1988; Hopkins & Bass, 1981). For example, when electrical waveforms mimicking female EODs are played to male mormyrids of the species *P. batesii*, experimental alterations to the signals on the scale of a few hundred microseconds change both Knollenorgan spike patterns and behavioural responses of the fish (Hopkins & Bass, 1981).

The present data illustrate how extraordinarily temporally precise and reliable Knollenorgan spike responses can be. The compound PSTHs measured here indicate that spike timing is reproducible, across thousands of stimulus repetitions, on time scales of ∼20 μs in *B. niger and G. petersii* and ∼4 μs in *P. adspersus*. Additionally, the result that these experimentally recorded spike times were well predicted by convolving the impulse response with the arbitrary stimulus provides evidence that the tuning properties of each Knollenorgan filter the stimulus linearly. This filtering in turn dictates spiking, with a brief latency to spike generation (<500 μs). Importantly, this linear transformation accurately represents temporal fluctuations of the stimulus into the 10–20 kHz range.

Although timing is extremely consistent, spike probability varies across trials, and is subject to the spike threshold non-linearity typical of most neurons with action potentials arising from voltage-dependent

conductances (Anderson et al., 2000; Hansel & van Vreeswijk, 2002; Troyer et al., 2002). Interestingly, Knollenorgans of *G. petersii* have been described as relatively insensitive to intensity, based on the observation that spike latency does not change with increased intensity, once threshold is crossed (Bell & Grant, 1989; Steinbach & Bennett, 1971). The present PSTHs, however, suggest an intensity sensitivity, at least in *B. niger*, that does not manifest itself as a change in spike timing but in spike probability, which greatly increases as intensity is raised; in fact, a supralinear increase in spike probability with intensity in *B. niger*, which cannot be attributed simply to spike threshold non-linearity, was the major source of unaccounted variance. An interesting but untested possibility is that the multiple sensory cells within the Knollenorgan are recruited or interact in some way to raise spike probability further than predicted by the simple model.

The temporal aspects of signals encoded at the periphery by Knollenorgans are transmitted centrally to the nucleus of the electrosensory lateral line lobe (NELL) and then to the toral nucleus exterolateralis pars anterior (ELa), where information about EOD signal is computed from comparisons of signal onset and offset (Friedman & Hopkins, 1998; Xu-Friedman & Hopkins, 1999). Timing information is preserved through specializations in the projections of Knollenorgan afferents, including synaptic contacts from the electroreceptor suited for electrotonic and/or ephaptic transmission with minimal delays, large axonal diameters, little branching, the absence of neuronal processes like dendrites, calyceal or large terminals at chemical synapses, and fixed-latency phasic (non-repetitive) spike responses to excitation in Knollenorgans, afferents, and NELL cells (Bell & Grant, 1989; Bennett, 1965; Friedman & Hopkins, 1998; Steinbach & Bennett, 1971; Tricas & Carlson, 2012). Interestingly many of the same properties, which all reduce temporal jitter in signal transmission, are present in time-encoding pathways for sound localization in auditory systems of birds and mammals (Carr & Konishi, 1990; Golding et al., 1995; Oertel, 1983, 1999; Raman & Trussell, 1992; Trussell, 1997).

Cellular mechanisms of high-frequency tuning in electroreceptors

The puzzle that persists is mechanistic. The present data demonstrate that Knollenorgans can behave as bandpass filters with high-frequency cut-offs above 10 kHz coupled with an electrical resonance, but the molecular identities and physiological mechanisms of the filters can only be definitively addressed by intracellular recordings from Knollenorgans of these species. The tuning of Knollenorgans of *B. brachyistius* has been modelled as a simple bandpass filter, in which a low-pass filtering RC circuit, representing the subthreshold behaviour of electrosensory cells, is embedded in the high-pass filtering capacitative arm of another RC circuit, composed of the resistance of the skin and the capacitance of the epithelial plug over the cells; the output predicted by such a circuit provides a reasonable approximation of tuning curves (Lyons-Warren et al., 2012). The same structures provide a plausible physical basis for the bandpass component of tuning seen in the present work.

B. brachyistius, however, has an EOD with relatively a low-frequency power spectrum (<5 kHz) and best frequencies <4 kHz in all Knollenorgans tested (Lyons-Warren et al., 2012). These features are distinct from the species studied here, which are closely related to each other (Peterson et al., 2022), and whose high-frequency EOD spectra motivated the present experiments. Moreover, tuning curves recorded here include >100 points over 2.5 log units of frequency. This high level of resolution showed that many Knollenorgans had tuning curves with inflexions or troughs, giving them a lobed or W-shape, indicative of mechanisms that increase responsiveness to a narrower subrange of frequencies than generated by a broad bandpass filter. A parallel observation is that the receptor potentials in Knollenorgans of *B. brachyistius* tend to be largely biphasic responses without resonance (Lyons-Warren et al., 2012). By contrast recordings in all species studied here typically included high-frequency, low-amplitude, damped oscillations during or after the spikes (noted or sketched in the laboratory notebook); at least two units in *B. niger* and *G. petersii* had damped oscillations nearly reaching the amplitude of the initial spike. Such incidental observations, coupled with the systematic appearance of inflexions in many tuning curves, raise the possibility that intrinsic properties of sensory cells amplify sensitivity in the region of the best frequency.

Given that electroreceptors either evolved from mechanosensitive hair cells or that the two cell classes have a common ancestor (Baker & Modrell, 2018), it is reasonable to look to hair cells for potential mechanisms. In direct recordings from turtle auditory hair cells, depolarizing currents evoke membrane potential resonance at frequencies that correspond to the best ('characteristic') frequency (Crawford & Fettiplace, 1980, 1981; Fettiplace & Crawford, 1980). In bullfrog saccular hair cells, turtle auditory hair cells, and chick auditory hair cells this resonance depends on two primary conductances: the depolarizing phase is driven by voltage-gated Ca currents that have the steepest region of their activation curves near the resting potential, and the repolarizing phase is driven by TEA-sensitive, Ca-activated BK currents with activation and deactivation kinetics that are more rapid in hair cells tuned to higher frequencies (Art & Fettiplace, 1987; Art et al., 1986, 1995;

Fuchs et al., 1988; Hudspeth & Lewis, 1988a, 1988b). The kinetics of the BK channels are regulated both by alternative splicing and by co-expression with beta subunits (Ramanathan et al., 1999, 2000). The resulting oscillations, however, barely exceed a few hundred hertz. Similarly, in electrosensory cells of ampullary organs of the little skate, a combination of voltage-gated Ca channels and BK channels can account for membrane potential oscillations observed in the ∼10 Hz range (Bellono et al., 2017; Clusin & Bennett, 1979a, 1979b).

If comparable ion channels were solely responsible for tuning of high-frequency Knollenorgans, they would require implausibly fast kinetics. Based on properties of known ion channels, the theoretical limit for electrical resonance has been calculated as <2 kHz (Fettiplace, 2020). Although some voltage-gated channels of cold-blooded animals gate in tens of microseconds even at room temperature (Hodgkin & Huxley, 1952; Markham & Zakon, 2014), it seems improbable that the membrane potential could fluctuate with a period of <100 μs. Instead it seems more likely that additional channel specializations, more complex combinations of conductances, and/or interactions among non-identical sensory cells within a single organ achieve high-frequency ringing beyond 5 kHz.

One distinctive feature of Knollenorgans is that, unlike hair cells, they fire spikes, the duration of which correlates with the best frequency (Bass & Hopkins, 1984). Like hair cells, however, they lack voltage-gated Na channels, suggesting that the spikes are supported by Ca currents (Lyons-Warren et al., 2012; Zipser & Bennett, 1973; see also Rutherford & Roberts, 2009). Well-timed firing evoked by specific high-frequency stimuli might be favoured by kinetic interactions among conductances activated at sub- and suprathreshold voltages, as in neurons with subthreshold intrinsic oscillations and/or spontaneous firing (Bal & McCormick, 1993, 1997; Bean, 2007; Huguenard & McCormick, 1992; Llinás & Mühlethaler, 1988; McCormick & Huguenard, 1992; Raman & Bean, 1999). Together such currents might produce the equivalent of an electrical resonance sufficient to account for the inflected tuning curves.

Beyond channel kinetics, the physical properties of Knollenorgans raise the possibility that electrical tuning is influenced by structural specializations of either the sensory cells or other components of the organ. In *G. petersii* the one to five sensory cells in each Knollenorgan are 35–40 μm diameter and are covered with microvilli 1–3 μm long (Derbin & Szabo, 1968). The microvilli presumably increase the capacitance greatly but also provide surface area for dense ion channel expression, which could drop membrane time constants into the millisecond or high microsecond range. Although short time constants would favour rapid voltage changes, they might also require large currents to reach threshold (Chen & von Gersdorff, 2019; Oertel, 1983; Trussell, 1999; Zhang & Trussell, 1994). The rapid rise and high magnitude of extracellularly recorded spikes suggest that the voltage-gated inward (likely Ca) current is indeed relatively large (Hopkins & Bass, 1981; Tricas & Carlson, 2012); likewise the phasic spike responses of Knollenorgans to sustained depolarization (Bennett, 1965) are indicative of large outward currents that render the cells leaky enough to counteract firing, as in auditory neurons (Golding et al., 1995; Rathouz & Trussell, 1998; Zhang & Trussell, 1994). High densities of voltage-gated currents may therefore provide high sensitivity by amplifying small input signals, as well as precise timing by driving suprathreshold responses that are rapid and brief.

The complex morphologies of sensory cells also raise the possibility of non-uniform channel expression. Subcellular compartmentalization of ion channel subtypes can make voltage excursions briefer and more well timed, as in the electric organ of *Steatogenys elegans* (Markham & Zakon, 2014). Such asymmetric distribution of specialized channels within or across sensory cells of a single Knollenorgan may facilitate responses to high-frequency signals.

Finally, structures auxiliary to the sensory cells may enhance tuning, as in the gecko (Beurg et al., 2022). Various features of Knollenorgans have been proposed to augment sensitivity to stimuli as small as a few hundred microvolts, including the high skin resistance, the impedance matching to the aquatic environment and possibly the serial capacitance of the epithelial plug that lies over the sensory cells (Bennett, 1965; Lyons-Warren et al., 2012). Whether these or other physical specializations help extend electrical tuning into the 10 kHz range has yet to be addressed.

References

Anderson, J. S., Lampl, I., Gillespie, D. C., & Ferster, D. (2000). The contribution of noise to contrast invariance of orientation tuning in cat visual cortex. *Science*, **290**(5498), 1968–1972.

Art, J. J., Crawford, A. C., & Fettiplace, R. (1986). Electrical resonance and membrane currents in turtle cochlear hair cells. *Hearing Research*, **22**, 31–36.

Art, J. J., & Fettiplace, R. (1987). Variation of membrane properties in hair cells isolated from the turtle cochlea. *The Journal of Physiology*, **385**, 207–242.

Art, J. J., Wu, Y. C., & Fettiplace, R. (1995). The calcium-activated potassium channels of turtle hair cells. *Journal of General Physiology*, **105**(1), 49–72.

Baker, C. V. H., & Modrell, M. S. (2018). Insights into electroreceptor development and evolution from molecular comparisons with hair cells. *Integrative and Comparative Biology*, **58**(2), 329–340.

Bal, T., & McCormick, D. A. (1993). Mechanisms of oscillatory activity in guinea-pig nucleus reticularis thalami in vitro: A mammalian pacemaker. *The Journal of Physiology*, **468**, 669–691

Bal, T., & McCormick, D. A. (1997). Synchronized oscillations in the inferior olive are controlled by the hyperpolarization-activated cation current I(h). *Journal of Neurophysiology*, **77**(6), 3145–3156.

Bass, A. H., & Hopkins, C. D. (1984). Shifts in frequency tuning of electroreceptors in androgen-treated mormyrid fish. *Journal of Comparative Physiology A*, **155**, 713–724.

Bean, B. P. (2007). The action potential in mammalian central neurons. *Nature Reviews Neuroscience*, **8**(6), 451–465.

Békésy, G. V. (1960). *Experiments in Hearing*. McGraw-Hill.

Bell, C. C. (1989). Sensory coding and corollary discharge effects in mormyrid electric fish. *Journal of Experimental Biology*, **146**, 229–253.

Bell, C. C. (1990). Mormyromast electroreceptor organs and their afferent fibers in mormyrid fish. III. Physiological differences between two morphological types of fibers. *Journal of Neurophysiology*, **63**(2), 319–332.

Bell, C. C., & Grant, K. (1989). Corollary discharge inhibition and preservation of temporal information in a sensory nucleus of mormyrid electric fish. *Journal of Neuroscience*, **9**(3), 1029–1044.

Bellono, N. W., Leitch, D. B., & Julius, D. (2017). Molecular basis of ancestral vertebrate electroreception. *Nature*, **543**(7645), 391–396.

Bellono, N. W., Leitch, D. B., & Julius, D. (2018).Molecular tuning of electroreception in sharks and skates. *Nature*, **558**(7708), 122–126.

Bennett, M. V. (1965). Electroreceptors in mormyrids. *Cold Spring Harbor symposia on quantitative biology*, **30**, 245–262.

Beurg, M., Tan, X., & Fettiplace, R. (2013). A prestin motor in chicken auditory hair cells: Active force generation in a nonmammalian species. *Neuron*, **79**(1), 69–81.

Beurg, M., Gamble, T., Griffing, A. H., & Fettiplace, R. (2022). Atypical tuning and amplification mechanisms in gecko auditory hair cells. *Proceedings of the National Academy of Sciences of the United States of America*, **119**(12), e2122501119.

Bialek, W., & Rieke, F. (1992). Reliability and information transmission in spiking neurons. *Trends in Neuroscience*, **15**(11), 428–434.

Bigorne, R. (1990). Révision systématique du genre Pollimyrus (Teleostei: Mormyridae) en Afrique de l'ouest. *Revue d'Hydrobiologie Tropicale*, **23**(4), 313–327.

Bigorne, R. (2003). Mormyridae. In D. Paugy, C. Lévêque, & G. G. Teugels (Eds.), *The fresh and brackish water fishes of west Africa* (pp. 122–184). Muséum national d'Histoire naturelle.

Blache, J. (1964). Les poissons du Bassin de Tchad et du Bassin Adjacent de Mayo Kebbi. Office de la recherche scientifique et technique. Outre-mer, Memoires, 30–57.

de Boer, E. (1968). Reverse correlation I: A heuristic introduction to the technique of triggered correlation, with applications to the analysis of compound systems. *Proceedings of the Koninklijke Nederlandse Akademie van Wetenschappen. Series C.*, **71**(5), 472–486.

de Boer, E. (1969). Reverse correlation. II. Initiation of nerve impulses in the inner ear. *Proceedings of the Koninklijke Nederlandse Akademie van Wetenschappen. Series C.*, **72**(2), 129–151.

de Boer, E., & de Jongh, H. R. (1978). On cochlear encoding: Potentialities and limitations of the reverse-correlation technique. *Journal of the Acoustical Society of America*, **63**(1), 115–135.

Boulenger, G. A. (1909). *Catalogue of the freshwater fishes of Africa in the British Museum Vol I and IV*. Longmans and Co.

Bullock, T. H., Behrend, K., & Heiligenberg, W. (1975). Comparison of the jamming avoidance responses in gymnotoid and gymnarchid electric fish: A case of convergent evolution of behavior and its sensory basis. *Journal of comparative physiology*, **103**, 97–121.

Carlson, B. A., Hasan, S. M., Hollmann, M., Miller, D. B., Harmon, L. J., & Arnegard, M. E. (2011). Brain evolution triggers increased diversification of electric fishes. *Science*, **332**(6029), 583–586.

Carr, C. E., & Konishi, M. (1990). A circuit for detection of interaural time differences in the brain stem of the barn owl. *Journal of Neuroscience*, **10**(10), 3227–3324.

Chen, M., & von Gersdorff, H. (2019). How to build a fast and highly sensitive sound detector that remains robust to temperature shifts. *Journal of Neuroscience*, **39**(37), 7260–7276.

Clusin, W. T., & Bennett, M. V. (1979a). The oscillatory responses of skate electroreceptors to small voltage stimuli. *Journal of General Physiology*, **73**(6), 685–702.

Clusin, W. T., & Bennett, M. V. (1979b). The ionic basis of oscillatory responses of skate electroreceptors. *Journal of General Physiology*, **73**(6), 703–723.

Crampton, W. G. R. (2019). Electroreception, electrogenesis and electric signal evolution. *Journal of Fish Biology*, **95**(1), 92–134.

Crawford, A. C., & Fettiplace, R. (1980). The frequency selectivity of auditory nerve fibres and hair cells in the cochlea of the turtle. *The Journal of Physiology*, **306**, 79–125.

Crawford, A. C., & Fettiplace, R. (1981). An electrical tuning mechanism in turtle cochlear hair cells. *The Journal of Physiology*, **312**, 377–412.

Crawford, J. D., & Huang, X. (1999). Communication signals and sound production mechanisms of mormyrid electric fish. *Journal of Experimental Biology*, **202**(Pt 10), 1417–1426.

Daget, J. (1954). Les poissons du Niger Supérieur. Memoires d'IFAN no 36.

Dallos, P. (1985). Response characteristics of mammalian cochlear hair cells. *Journal of Neuroscience*, **5**(6), 1591–1608.

Dallos, P., & Evans, B. N. (1995). High-frequency motility of outer hair cells and the cochlear amplifier. *Science*, **267**(5206), 2006–2009.

Derbin, C., & Szabo, T. (1968). Ultrastructure of an electroreceptor (Knollenorgan) in the Mormyrid fish Gnathonemus petersii. I. *Journal of Ultrastructure Research*, **22**(5), 469–484.

Engelmann, J., Gertz, S., Goulet, J., Schuh, A., & von der Emde, G. (2010). Coding of stimuli by ampullary afferents in Gnathonemus petersii. *Journal of Neurophysiology*, **104**(4), 1955–1968.

Fettiplace, R. (2020). Diverse mechanisms of sound frequency discrimination in the vertebrate cochlea. *Trends in Neuroscience*, **43**(2), 88–102.

Fettiplace, R., & Crawford, A. C. (1980). The origin of tuning in turtle cochlear hair cells. *Hearing Research*, **2**(3–4), 447–454.

Friedman, M. A., & Hopkins, C. D. (1998). Neural substrates for species recognition in the time-coding electrosensory pathway of mormyrid electric fish. *Journal of Neuroscience*, **18**(3), 1171–1185.

Fuchs, P. A., & Evans, M. G. (1988). Voltage oscillations and ionic conductances in hair cells isolated from the alligator cochlea. *Journal of Comparative Physiology A*, **164**(2), 151–163.

Fuchs, P. A., Nagai, T., & Evans, M. G. (1988). Electrical tuning in hair cells isolated from the chick cochlea. *Journal of Neuroscience*, **8**(7), 2460–2467.

Golding, N. L., Robertson, D., & Oertel, D. (1995). Recordings from slices indicate that octopus cells of the cochlear nucleus detect coincident firing of auditory nerve fibers with temporal precision. *Journal of Neuroscience*, **15**(4), 3138–3153.

Günther, A. (1862) Eine neue art von Mormyrus. *Archiv für Naturgeschichte*, **28**, 64.

Günther, A. (1866). *Catalogue of the fishes in the British Museum*. Catalogue of the Physostomi, containing the families Salmonidae, Percopsidae, Galaxidae, Mormyridae, Gymnarchidae, Esocidae, Umbridae, Scombresocidae, Cyprinodontidae, in the collection of the British Museum pp. 219, 221.

Hansel, D., & van Vreeswijk, C. (2002). How noise contributes to contrast invariance of orientation tuning in cat visual cortex. *Journal of Neuroscience*, **22**(12), 5118–5128.

Harder, W. (1968). Die beziehungen zwischen elektrorezeptoren, Elektrischem Organ, seitenlinienorganen und nervensystem bei den Mormyridae (Teleostei, Pisces). *Zeitschrift für Vergleichende Physiologie*, **59**, 272–318.

Hodgkin, A. L., & Huxley, A. F. (1952). A quantitative description of membrane current and its application to conduction and excitation in nerve. *The Journal of Physiology*, **117**(4), 500–544.

Hopkins, C. D. (1976) Stimulus filtering and electroreception: Tuberous electroreceptors in three species of gymnotoid fish. *Journal of comparative physiology*, **111**(2), 171–207.

Hopkins, C. D. (1981) On the diversity of electric signals in a community of mormyrid electric fish in West Africa. *American Zoologist*, **21**(1), 211–222.

Hopkins, C. D. (1988). Neuroethology of electric communication. *Annual Review of Neuroscience*, **11**, 497–535.

Hopkins, C. D., & Bass, A. H. (1981) Temporal coding of species recognition signals in an electric fish. *Science*, **212**(4490), 85–87.

Hudspeth, A. J., & Lewis, R. S. (1988a). Kinetic analysis of voltage- and ion-dependent conductances in saccular hair cells of the bull-frog, *Rana catesbeiana*. *The Journal of Physiology*, **400**, 237–274.

Hudspeth, A. J., & Lewis, R. S. (1988b). A model for electrical resonance and frequency tuning in saccular hair cells of the bull-frog, *Rana catesbeiana*. *The Journal of Physiology*, **400**, 275–297.

Huguenard, J. R., & McCormick, D. A. (1992). Simulation of the currents involved in rhythmic oscillations in thalamic relay neurons. *Journal of Neurophysiology*, **68**(4), 1373–1283.

Llinás, R., & Mühlethaler, M. (1988). An electrophysiological study of the in vitro, perfused brain stem-cerebellum of adult guinea-pig. *The Journal of Physiology*, **404**, 215–40.

Lyons-Warren, A. M., Hollmann, M., & Carlson, B. A. (2012). Sensory receptor diversity establishes a peripheral population code for stimulus duration at low intensities. *Journal of Experimental Biology*, **215**(Pt 15), 2586–2600.

Markham, M. R., & Zakon, H. H. (2014). Ionic mechanisms of microsecond-scale spike timing in single cells. *Journal of Neuroscience*, **34**(19), 6668–6678.

McCormick, D. A., & Huguenard, J. R. (1992). A model of the electrophysiological properties of thalamocortical relay neurons. *Journal of Neurophysiology*, **68**(4), 1384–1400.

McKibben, J. R., Hopkins, C. D., & Yager, D. D. (1993). Directional sensitivity of tuberous electroreceptors: Polarity preferences and frequency tuning. *Journal of Comparative Physiology A*, **173**, 415–424.

Nawar, G. (1959). Observations on breeding of six members of the Nile Mormyridae. *Journal of Natural History*, **2**(20), 493–504.

Oertel, D. (1983). Synaptic responses and electrical properties of cells in brain slices of the mouse anteroventral cochlear nucleus. *Journal of Neuroscience*, **3**(10), 2043–2053.

Oertel, D. (1999). The role of timing in the brainstem auditory nuclei of vertebrates. *Annual Review of Physiology*, **61**, 497–519.

Peterson, R. D., Sullivan, J. P., Hopkins, C. D., Santaquiteria, A., Dillman, C. B., Pirro, S., Betancur-R, R., Arcila, D., Hughes, L. C., & Ortí, G. (2022). Phylogenomics of bony-tongue fishes (Osteoglossomorpha) shed light on craniofacial evolution and biogeography of the weakly electric clade (Mormyridae). *Systematic Biology*, **71**(5) 1032–1044.

Pezzanite, B., & Moller, P. (1998). A sexually dimorphic basal anal-fin ray expansion in the weakly discharging electric fish *Gnathonemus petersii*. *Journal of Fish Biology*, **53**(3), 638–644.

Pitchford, S., & Ashmore, J. F. (1987). An electrical resonance in hair cells of the amphibian papilla of the frog Rana temporaria. *Hearing Research*, **27**(1), 75–83.

Quinet, P. (1971). Etude systématique des organes sensoriels de la peau des Mormyriformes. *Musée Royal de l'Afrique Centrale, Tervuren, Belgique, Documentation Zoologique*, **190**, 1–97.

Raman, I. M., & Bean, B. P. (1999). Ionic currents underlying spontaneous action potentials in isolated cerebellar Purkinje neurons. *Journal of Neuroscience*, **19**(5), 1663–1674.

Raman, I. M., & Trussell, L. O. (1992). The kinetics of the response to glutamate and kainate in neurons of the avian cochlear nucleus. *Neuron*, **9**(1), 173–86.

Ramanathan, K., Michael, T. H., Jiang, G. J., Hiel, H., & Fuchs, P. A. (1999). A molecular mechanism for electrical tuning of cochlear hair cells. *Science*, **283**(5399), 215–217.

Ramanathan, K., Michael, T. H., & Fuchs, P. A. (2000). Beta subunits modulate alternatively spliced, large conductance, calcium-activated potassium channels of avian hair cells. *Journal of Neuroscience*, **20**(5), 1675–1684.

Rathouz, M., & Trussell, L. (1998). Characterization of outward currents in neurons of the avian nucleus magnocellularis. *Journal of Neurophysiology*, **80**(6), 2824–2835.
Rutherford, M. A., & Roberts, W. M. (2009). Spikes and membrane potential oscillations in hair cells generate periodic afferent activity in the frog sacculus. *Journal of Neuroscience*, **29**(32), 10025–10037.
Saunders, A. N., & Gallant, J. R. (2024). A review of the reproductive biology of mormyroid fishes: An emerging model for biomedical research. *Journal of experimental zoology. Part B, Molecular and developmental evolution*, **342**(3), 144–163.
Smotherman, M. S., & Narins, P. M. (1999). The electrical properties of auditory hair cells in the frog amphibian papilla. *Journal of Neuroscience*, **19**(13), 5275–5292.
Steinbach, A. B., & Bennett, M. V. (1971). Effects of divalent ions and drugs on synaptic transmission in phasic electroreceptors in a mormyrid fish. *Journal of General Physiology*, **58**(5), 580–598.
Tan, X., Beurg, M., Hackney, C., Mahendrasingam, S., & Fettiplace, R. (2013) Electrical tuning and transduction in short hair cells of the chicken auditory papilla. *Journal of Neurophysiology*, **109**(8), 2007–2020.
Tricas, T. C., & Carlson, B. A. (2012). Electroreceptors and magnetoreceptors. In *Cell Physiology Sourcebook* (pp. 705–725). Elsevier. https://doi.org/10.1016/B978-0-12-387738-3.00041-X
Troyer, T. W., Krukowski, A. E., & Miller, K. D. (2002). LGN input to simple cells and contrast-invariant orientation tuning: An analysis. *Journal of Neurophysiology*, **87**(6), 2741–2752.
Trussell, L. O. (1997). Cellular mechanisms for preservation of timing in central auditory pathways. *Current Opinion in Neurobiology*, **7**(4), 487–492.
Trussell, L. O. (1999). Synaptic mechanisms for coding timing in auditory neurons. *Annual Review of Physiology*, **61**, 477–496.
Watson, D., & Bastian, J. (1979). Frequency response characteristics of electroreceptors in the weakly electric fish, *Gymnotus carapo*. *Journal of comparative physiology*, **134**(3), 191–202.
Wu, Y. C., Art, J. J., Goodman, M. B., & Fettiplace, R. (1995). A kinetic description of the calcium-activated potassium channel and its application to electrical tuning of hair cells. *Progress in Biophysics and Molecular Biology*, **63**(2), 131–158.
Xu-Friedman, M. A., & Hopkins, C. D. (1999). Central mechanisms of temporal analysis in the Knollenorgan pathway of mormyrid electric fish. *Journal of Experimental Biology*, **202**(10), 1311–1318.
Zhang, S., & Trussell, L. O. (1994). Voltage clamp analysis of excitatory synaptic transmission in the avian nucleus magnocellularis. *The Journal of Physiology*, **480**(1), 123–136.
Zheng, J., Shen, W., He, D. Z., Long, K. B., Madison, L. D., & Dallos, P. (2000). Prestin is the motor protein of cochlear outer hair cells. *Nature*, **405**(6783), 149–155.
Zipser, B., & Bennett, M. V. (1976). Responses of cells of posterior lateral line lobe to activation of electroreceptors in a mormyrid fish. *Journal of Neurophysiology*, **39**(4), 693–712.
Zipser, B., & Bennett, M. V. (1973). Tetrodotoxin resistant electrically excitable responses of receptor cells. *Brain Research*, **62**(1), 253–259.

Additional information

Data availability statement

Data will be made available upon request to the authors.

Competing interests

The authors declare that they have no competing interests.

Author contributions

C.D.H. conceived of the project. I.M.R. acquired the data and wrote the manuscript. I.M.R. and C.D.H. performed the analysis, interpreted the data and edited the manuscript. Both authors approved the final manuscript and agreed to be accountable for all aspects of the work. Both persons designated as authors qualify for authorship, and all those who qualify for authorship are listed.

Funding

This work was supported by National Institutes of Health NIH MH37972 (C.D.H.) and NS116854 (I.M.R.).

Acknowledgements

We are grateful to Garry Harned (1935–2022) for his technical support and guidance to I.M.R. throughout the project, and we thank J.D. Crawford for the recordings of EODs. We are also indebted to Prof. Robert Fettiplace for his encouragement to revisit and communicate this work.

Keywords

auditory hair cell, electrical resonance, reverse correlation, tuberous electroreceptor

Supporting information

Additional supporting information can be found online in the Supporting Information section at the end of the HTML view of the article. Supporting information files available:

Peer Review History